COPPE
Instituto Alberto Luiz Coimbra de Pós-Graduação e Pesquisa de Engenharia
UFRJ

MULTIVARIABLE SLIDING MODE BASED EXTREMUM SEEKING VIA MONITORING OR PERIODIC SWITCHING FUNCTIONS

Nerito Oliveira Aminde

Tese de Doutorado apresentada ao Programa de Pós-graduação em Engenharia Elétrica, COPPE, da Universidade Federal do Rio de Janeiro, como parte dos requisitos necessários à obtenção do título de Doutor em Engenharia Elétrica.

Orientadores: Liu Hsu
Tiago Roux de Oliveira

Rio de Janeiro
Dezembro de 2021

MULTIVARIABLE SLIDING MODE BASED EXTREMUM SEEKING VIA MONITORING OR PERIODIC SWITCHING FUNCTIONS

Nerito Oliveira Aminde

TESE SUBMETIDA AO CORPO DOCENTE DO INSTITUTO ALBERTO LUIZ COIMBRA DE PÓS-GRADUAÇÃO E PESQUISA DE ENGENHARIA DA UNIVERSIDADE FEDERAL DO RIO DE JANEIRO COMO PARTE DOS REQUISITOS NECESSÁRIOS PARA A OBTENÇÃO DO GRAU DE DOUTOR EM CIÊNCIAS EM ENGENHARIA ELÉTRICA.

Orientadores: Liu Hsu
Tiago Roux de Oliveira

Aprovada por: Prof. Liu Hsu
Prof. Tiago Roux de Oliveira
Prof. Alessandro Jacoud Peixoto
Prof. Daniel Ferreira Coutinho
Prof. Aldayr Dantas de Araújo

RIO DE JANEIRO, RJ – BRASIL
DEZEMBRO DE 2021

Aminde, Nerito Oliveira

Multivariable Sliding Mode Based Extremum Seeking via Monitoring or Periodic Switching Functions/Nerito Oliveira Aminde. – Rio de Janeiro: UFRJ/COPPE, 2021.

XIII, 69 p.: il.; 29, 7cm.

Orientadores: Liu Hsu

Tiago Roux de Oliveira

Tese (doutorado) – UFRJ/COPPE/Programa de Engenharia Elétrica, 2021.

Referências Bibliográficas: p. 63 – 69.

1. Extremum Seeking Control. 2. Sliding Mode Control. 3. Monitoring Function. 4. Periodic Switching Function. 5. Multivariable Nonlinear Systems. I. Hsu, Liu *et al.* II. Universidade Federal do Rio de Janeiro, COPPE, Programa de Engenharia Elétrica. III. Título.

Às minhas filhas Aisha
(in memorian 👼🏾) e Ayla e
à minha irmã Janete (in memorian)

Acknowledgements

Agradeço primeiramente a Deus, meu orientador primordial, responsável por todas as metamorfoses da minha vida que culminaram com esse feito inédito, um menino simples sonhador da Maganja da Costa se tornar Doutor em Engenharia Elétrica pela UFRJ!

Agradeço especialmente ao meu orientador Prof. Emérito Liu Hsu e coorientador Prof. Tiago Roux de Oliveira, que me acompanharam desde o mestrado e graduação, respectivamente, por seus valiosos ensinamentos que transcendem as fronteiras acadêmicas. Suas críticas construtivas, rigor matemático, perícia e paciência foram imprescindíveis para a materialização desta tese, perante algumas fragilidades e adversidades.

Aos Professores Fernando Lizarralde e Ramon Costa por tornar o Labcon um espaço agradável de troca de conhecimento com bom humor. Ademais, remerceio aos Professores Alessandro Jacoud Peixoto, Daniel Coutinho e Aldayr Araújo, por aceitarem participar da banca, trazendo valiosas contribuições para o aprimoramento da tese.

Um agradecimento especialíssimo vai para minha amada esposa Josenice Aminde e à nossa filha AYLA, pelo amor, amizade, carinho e suporte incondicional, além da compreensão por quase cinco anos divididos entre elas e o doutorado. Amo vocês!

Aos meus estimados pais Oliveira e Betinha, irmãos Chinoca, Ronaldo, Zito e Ivanildo; tios, primos, sobrinhos e amigos, que apesar da distância entre o Brasil e Moçambique, contribuíram indiretamente nesse grande feito, através dos contactos frequentes e orações.

Gratulo aos colegas do curso e demais amigos no Brasil, Filipe, Claver, João, Marcel, Marcus, Thales, Alessandro Santos, Diego Dias, Edison Alfaro, Denise Alves, Joaquim, Germildo, Teodósio Nzualo, Vithor Nypwipwy, Gilmara Carvalho, Carlos Subuhana, Gil Vicente, entre tantos outros, que tornaram fácil a vida na diáspora e contribuíram multidimensionalmente para lograr os meus objetivos.

Por fim, e não menos importante, agracio fundamentalmente ao Instituto Superior Dom Bosco (ISDB) em Moçambique, que em parceria com a NUFFIC/CINOP Global (Holanda) financiaram os meus estudos.

"DHINOUTAMALELANI MWETENE!"

Abstract of Thesis presented to COPPE/UFRJ as a partial fulfillment of the requirements for the degree of Doctor of Science (D.Sc.)

CONTROLE EXTREMAL MULTIVARIÁVEL POR MODOS DESLIZANTES VIA FUNÇÃO DE MONITORAÇÃO OU FUNÇÃO DE CHAVEAMENTO PERIÓDICA

Nerito Oliveira Aminde

December/2021

Advisors: Liu Hsu
Tiago Roux de Oliveira

Department: Electrical Engineering

In this thesis, two novel methods of extremum seeking control based on sliding modes and output feedback for real-time optimization of a class of uncertain nonlinear multivariable systems are introduced. Specifically, the methods are: (1) extremum seeking control based on the monitoring function and cyclic search and (2) extremum seeking control based on the periodic switching function and cyclic search. In the former approach, static and dynamic maps are considered, and in the latter only static maps. It is ensured, in both approaches, that the objective functions reach, in real-time, a small neighborhood of their optimal operating or equilibrium points. For dynamic mappings with arbitrary relative degree, singular perturbation and time-scaling techniques are employed. The stability and convergence analysis for the monitoring function-based scheme is done through point transformations called parabolic-recurrence method, while the periodic switching function is based on the Lyapunov's stability theory. The obtained results indicate that the proposed control strategies allow for achieving global convergence and stability properties, while in the literature such properties are only local or semi-global. Numerical simulations corroborate with the theoretical results.

Resumo da Tese apresentada à COPPE/UFRJ como parte dos requisitos necessários para a obtenção do grau de Doutor em Ciências (D.Sc.)

Nerito Oliveira Aminde

Dezembro/2021

Orientadores: Liu Hsu
Tiago Roux de Oliveira

Programa: Engenharia Elétrica

Nesta tese, são apresentados dois novos métodos de controle por busca extremal para a otimização em tempo real de uma classe de sistemas multivariáveis não-lineares incertos, através do controle por modos deslizantes e realimentação de saída. Especificamente, os métodos são: (1) controle extremal baseado em função de monitoração e busca cíclica e (2) controle extremal baseado em função de chaveamento periódica e busca cíclica. No primeiro, são considerados mapeamentos estáticos e dinâmicos e no segundo apenas mapeamentos estáticos, sendo garantido, em ambas abordagens, que as funções-objetivo alcançam, em tempo real, uma vizinhança pequena de seus pontos ótimos de operação ou de equilíbrio. Para mapeamentos dinâmicos com grau relativo arbitrário, utilizam-se as técnicas de perturbação singular e escalonamento do tempo. A análise de estabilidade e convergência para o controle via função de monitoração é feita por transformações pontuais que denominamos método de recorrências parabólicas, ao passo que a abordagem via função de chaveamento periódica, baseia-se na teoria de estabilidade de Lyapunov. Resultados da pesquisa indicam que as estratégias de controle propostas permitem alcançar propriedades de convergência e estabilidade globais, enquanto na literatura tem-se convergência e estabilidade locais ou semi-globais. Simulações numéricas corroboram os resultados teóricos.

Sumário

Lista de Figuras

List of Abbreviations

SISO	Single-Input Single-Output
MISO	Multiple-Input Single-Output
MIMO	Multiple-Input Multiple-Output
ESC	Extremum Seeking Control
MESC	Multivariable Extremum Seeking Control
HFG	High-Frequency Gain
VSC	Variable Structure Control
SMC	Sliding Mode Control
GAS	Globally Asymptotically Stable

Capítulo 1

Introduction

Optimization is the primary motivation for all reasonable human actions. It is utilized in our daily lives without notice. In general, through our actions, we are interested in achieving a particular state in which a specific objective is optimal (maximized or minimized) [3]. Similarly, real-time optimization is one of the objectives of any control system [4].

A popular real-time optimization technique is extremum seeking, originally proposed in France by Leblanc in 1922. It is a feedback control technique aimed to find operating set-points that optimizes an uncertain objective function [5]. Extremum seeking is applicable in situations where there is a nonlinear objective map in the control problem, and the nonlinearity has a local minimum or a maximum.

Real-time optimization is a difficult problem, specially if little or no model information is known a priori. However, these problems can be interpreted under the light of trajectory tracking control and the existing literature shows promising results for single-input single-output (SISO) systems [6–8] and multi-input single-output (MISO) systems [9, 10]. In this thesis, we aim to develop multivariable sliding mode based extremum seeking controllers through monitoring function or periodic switching function and output feedback to optimize uncertain nonlinear objective functions.

Control of Uncertain Nonlinear Systems

A typical feedback control system is illustrated in Figure 1.1. Feedback control systems of this form can be divided into two main classes: output feedback and state feedback, the later require all state to be measured for implementation, which is physically difficult or economically expensive, so in this work we will deal only with output feedback. However, output feedback design is simplified only for systems with relative degree one. For systems with relative degree greater than one, the use of state estimation schemes is required. Therefore, in order to keep an output

feedback control law, state observers must be implemented to produce estimates of the unmeasured states.

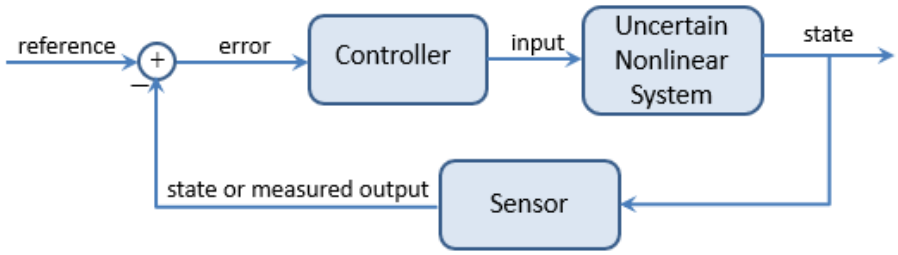

Figura 1.1: Typical feedback control system

Regarding uncertainties in dynamic systems (linear or nonlinear), robust and adaptive control are the main strategies in the literature for dealing with systems that have poor modeling, including parametric variations [11].

The main topic of research in this thesis is extremum seeking control (ESC), which is an adaptive control methodology that optimizes the steady-state performance of a plant by automatically adjusting its inputs [9]. On the other hand, sliding mode variable structure control or simply sliding mode control (SMC) is a very efficient robust control alternative for controlling uncertain systems [6, 11]. Thus, we want to design controllers based on sliding mode control and output feedback to address with uncertain nonlinear systems in optimization problems, leading to global or semi-global solutions. The term global [12] refers to a stability or tracking task that is achieved independently of the initial conditions of the closed-loop system, while semi-global refers to a property obtained from a compact set of initial conditions, that can be arbitrarily increased by tuning some controller parameter.

1.1 Objectives

The objective of this thesis is to develop sliding mode control laws for uncertain nonlinear systems, based on two approaches, (1) monitoring function with cyclic search and (2) periodic switching function with cyclic search. Specifically, we want to design new global solutions for real-time optimization of uncertain multivariable nonlinear systems under unknown control direction (unknown gradient and Hessian). Monitoring function and periodic switching functions are designed to cope with the lack of the control direction knowledge, while sliding mode is used to solve the problem of system uncertainties. On the other hand, cyclic search is introduced to reduce the multivariable problem to a sequence of scalar sub-problems. Thus, we expand the applicability of our previous results for static maps [13, 14] and dynamic

maps [15]. The proposed control designs are followed by the stability analysis based on the so-called *Parabolic Recurrence Method* [16], and nonlinear system's analysis tools, such as Lyapunov stability theory and singular perturbation theory.

To the best of our knowledge, it is the first time that multivariable sliding mode based extremum seeking control via monitoring function is introduced in the literature. On the other hand, the earlier approach, based on periodic switching function has been proposed in the literature [2, 17], however, we have relaxed some assumptions and make some modifications in the control loop, which improves its performance, as will be shown throughout the thesis (chapter 3).

1.2 Literature Review

To cover a brief literature review, in the following sections three advanced control theory techniques are presented, within the scope of this thesis, namely Adaptive Control and Extremum Seeking Control with or without sliding modes.

1.2.1 Adaptive Control

The concept of adaptive system and adaptive control dates back to the 1950s [18] and it is still an active research topic [19]. According to Ioannou and Fidan [20], adaptive control is the combination of a parameter estimator, which generates parameter estimates online, with a control law in order to control classes of plants whose parameters are completely unknown and/or could change with time unpredictably.

Adaptive control can be divided into three main classes, as illustrated in Figure 1.2: the classical model-based adaptive control (MRAC - Model Reference Adaptive Control), which mainly uses physics-based models of the controlled system; the model-free adaptive control, which is solely based on the interaction of the controller with the system; and learning-based adaptive control, which uses both model-based and model-free techniques to design flexible yet fast and stable adaptive controllers. Extremum seeking control belongs to the class of model-free adaptive controllers, that allow a lot of flexibility in terms of model structures because they do not rely on any model. However, they lack some of the stability guarantees which characterize model-based adaptive controllers.

Depending on the approach used to compensate the model uncertainties, model-based adaptive control can be classified either in direct MRAC or indirect MRAC. On the other hand, in terms of the nature of the model and the controller equations, it can be classified as linear controllers (continuous or discrete) or nonlinear controllers (continuous or discrete). For convenience, we will not present the details of the subclasses of either model-based adaptive control or learning-based adaptive control.

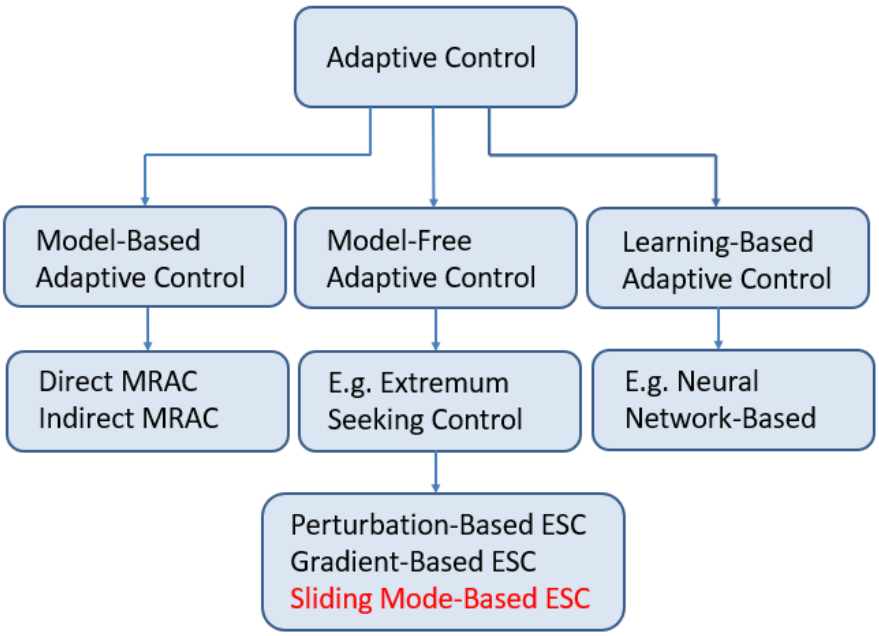

Figura 1.2: Three main streams of Adaptive Control: model-based, model-free, and learning-based adaptive control. Sliding Mode based ESC is the main topic in this thesis.

As told before, extremum seeking control is an example of a model-free adaptive control, which will be described in the next section. Another example of a model-free adaptive control is reinforcement learning algorithms, which is a class of machine learning algorithms and learns how to map states to actions in such a way to maximize a desired reward. However, ESC is more powerful (learning online, in one experiment, not through numerous tests) but this is still understood by too few as an advantage over machine and reinforcement learning.

1.2.2 Extremum Seeking Control

There are many problems of engineering for which an optimal operating point or condition exists, but this point or condition is not necessarily well known or easy to find. ESC belongs to a family of control design methods whose purpose is to automatically find an optimal system behavior (e.g., equilibrium point or trajectory to be tracked) for the closed-loop system, while at the same time maintaining stability and boundedness of signals. ESC is therefore mainly used to perform real-time optimization (RTO) for dynamic systems [21].

ESC can be categorized in different manners [21, 22], for instance, in [21] it is categorized into two main groups: analog (continuous) optimization-based extremum seeking control (AOESC) and numerical (discrete) optimization-based extremum seeking control (NOESC). Analog optimization-based methods includes gradient based

design (GESC), perturbation-based design (PESC) and sliding mode based design (SMESC). The following section briefly describes Analog optimization-based algorithms, which are our object of study.

Perturbation-based ESC and Gradient-based ESC

According to Reference [4], the idea behind the perturbation-based approach, which is the most popular, is to add a small probing signal (sometimes called dither signal) to a base input (u), and then measure the change in the output (y) with respect to this signal. Based on this change, it will be decided to increase or decrease the input signal (u).

Extremum seeking control received great attention from the control community after the work of Krstić and Wang [23] in 2000, which established the first rigorous stability proof for this perturbation-based design, based on standard averaging and singular perturbation theory, which guarantees at least local convergence. Since then, many significant theoretical results on stability and performance aspects have been published by several authors. This section highlights some contributions of these works, according to the aforementioned branches. For each ESC branch, there is a scalar and multivariable approach, as well as a continuous time and discrete-time method.

Since 2000, significant theoretical advances on ESC were carried out, such as the generalization for multi-input-multi-output (MIMO) plants [24], semi-global convergence proof [25], extension for multi-input-single-output (MISO) maps with output delays [26] and input delays [27]. Please, refer to Table 1 for more references.

In what follows, we present an intuitive description of the perturbation-based ESC. For details, the reader can refer to [5] and [28].

Consider a dynamic system given by

$$\dot{x} = f(x, u) \tag{1.1}$$

$$y = h(x), \tag{1.2}$$

where u is parameterized by θ, i.e., $u = \alpha(x, \theta)$, assuming that there is an unique equilibrium map $l(\theta)$ such that $\dot{x} = 0$ if and only if $x = l(\theta)$, and the unknown output $y = h(x)$ has a maximum at some value $\theta = \theta^*$.

Figure 1.3 illustrates the perturbation-based control scheme. The dither term $a\sin(\omega t)$ is used to perturb the value of θ, in order to search for the optimal control which maximize the output function y. The value of the output function, $y = h(x)$, is first passed through the high-pass filter, whose Laplace transform is represented as $\dfrac{s}{s+\omega_h}$ in order to remove any constant terms. The filtered signal is then mixed with the same term, $a\sin(\omega t)$, and then low-pass filtered, a process which after

some averaging analysis results in few oscillating terms, one of which is of the form $sin^2(\omega t)$ and proportional to $\frac{dh}{d\theta}$, the gradient of the unknown output map. Upon integration, or low-pass filtering through $-\frac{k}{s}$ all oscillatory terms has zero average, except the term $k\frac{dh}{d\theta}\sin^2(\omega t)$, resulting in θ following a gradient ascent towards the maximizer value θ^* of the unknown function $y = h(x)$.

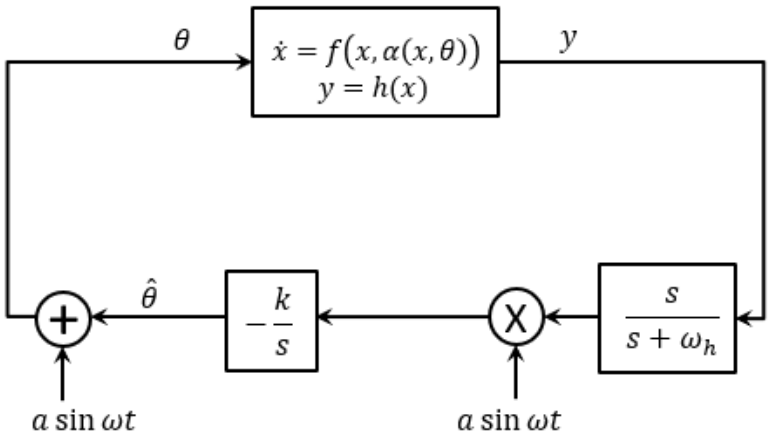

Figura 1.3: Gradient-based ESC

On the other hand, considering the same system (1.1)-(1.2), the gradient-based ESC [19] is defined as follows:

$$\dot{\theta} = k\frac{dh}{d\theta}, \quad k > 0, \tag{1.3}$$

which convergence can be analyzed using the following Lyapunov function

$$V = h(\theta^*) - h(\theta) > 0, \quad \text{for} \quad \theta \neq \theta^*. \tag{1.4}$$

The derivative of V *w.r.t.* time results in

$$\dot{V} = -\frac{dh}{d\theta}\dot{\theta} = -k\left(\frac{dh}{d\theta}\right)^2 \leq 0, \tag{1.5}$$

which proves that (1.3) drives θ to the invariant set such that $\frac{dh}{d\theta} = 0$, i.e., $\theta = \theta^*$. It is clear from (1.3), the dependence of the algorithm on the gradient of the output function h. This dependence can be overcome by the sliding mode control technique, which is introduced in the next section.

Sliding mode based ESC

The concept of sliding mode control dates back to the 1960s, and it is still an active research topic. The sliding mode control (SMC) is recognized as one of the efficient tools to design robust controllers for complex high-order nonlinear dynamic plants operating under uncertainty conditions. SMC is a special class of the variable-structure systems (VSS). The sliding mode control method alters the dynamics of a given dynamical system (linear or nonlinear) by applying a discontinuous control signal that forces the system to slide along a cross-section (manifold) of the systems of normal behavior [29].

The main advantage of the sliding mode controllers is their insensitivity to parameter variations and disturbances during the sliding mode, thus eliminating the requirement of the exact modeling. The SMC design is composed of two steps:

- In the first step, a sliding surface should be properly designed. While on the sliding surface, the plant dynamics is restricted to the equations of the surface, being robust to matched plant uncertainties and external disturbances.

- In the second step, a feedback control law should be designed to provide convergence of the system trajectories to the sliding surface; thus, the sliding surface should be reached in a finite time. The system's motion on the sliding surface is called the *sliding mode*.

Important types of SMC [29] are: classical sliding mode control (first-order sliding mode control, FOSMC), integral sliding mode control (ISMC), higher-order sliding mode control (HOSMC), terminal sliding mode control (TSMC), and super-twisting sliding mode control (STSMC). Fundamental design and analysis tools used in classical SMC are discussed by Utkin [30]. According to Shtessel et al. [31], ISMC has the properties of retaining the order of the compensated system's dynamics in the sliding mode and disturbance compensation while the HOSM control has the ability to drive the sliding variable and its $k-1$ successive derivatives (a so-called kth-order sliding mode) to zero in finite time. The STSMC can be understood as a PID controller with nonlinear proportional and integral actions. TSMC is designed to achieve finite-time convergence of the state to the origin after the reaching phase.

Sliding mode control has been successfully applied to robot manipulators, underwater vehicles [32], automotive transmissions and engines, high-performance electric motors, and power systems [33]. In control theory, SMC is applied to other problems such as regulation, observers, output feedback and trajectory tracking [34]. The latter two problems are considered in this thesis, i.e., first order SMC applied to extremum seeking control through output feedback and trajectory tracking.

The design of controllers by output feedback of uncertain systems without the knowledge of the high frequency gain has been an intriguing problem since the

1980s. In adaptive control, the so-called Nussbaum gain has been used in an attempt to relax this hypothesis [11, 35]. However, this approach is controversial from a practical point of view due to large transients, excessive control effort and consequent lack of robustness [35].

Lately, controllers based on output feedback and sliding modes for tracking uncertain, linear and non-linear SISO systems with unknown control direction were introduced in [36] and [37], respectively. In place of Nussbaum gain, the control direction was adjusted from monitoring functions.

In variable structure MRAC, the MRAC reference model control structure is used. The integral laws of adaptation are replaced by switched laws, resulting in a switched control signal, as in the variable structure systems ([38], [39], [40]). Despite the good transient performance, in general, there is the presence of the phenomenon of "chattering"

Recalling the system (1.1)-(1.2), it was demonstrated in the previous section that gradient-based ESC needs the knowledge of the gradient of the objective function, thus, using the concepts of SMC, we now show how to develop a sliding mode based ESC, introduced by Korovin and Utkin [41], by defining a tracking error

$$e = h(\theta(t)) - h_{ref}(t), \tag{1.6}$$

where $h_{ref}(t)$ denotes a time function, which is monotonically increasing, in case of maximization problems. The idea is that if h tracks h_{ref}, then it will increase until it reaches an invariant set centered around the equality $\dfrac{dh}{d\theta} = 0$. A simple way to achieve this goal is by choosing the following extremum seeking law, named as Drakunov-Özgüner's periodic switching function [42]:

$$\dot{\theta} = k_1 \operatorname{sgn}\left(\sin\left(\frac{\pi e}{k_2}\right)\right), \quad k_1,\ k_2 > 0. \tag{1.7}$$

Figure 1.4 illustrate such a sliding mode control scheme. With this controller, at least one of the sliding surfaces, $e(t) = kk_2$, with k odd or even, would be a stable sliding surface, independent of the control direction. Moreover, this controller is shown to steer θ to the set such that $\dfrac{dh}{d\theta} < \dfrac{\dot{h}_{ref}}{k_1}$, which can be made arbitrarily small by the proper tuning of k_1. In [43], the authors enhanced the sliding mode ESC approach by utilizing an output-feedback version of the Drakunov-Özgüner periodic switching function. The authors proved that global exact tracking was achievable for uncertain plants with unknown control direction, and then employed it for extremum seeking of SISO systems.

Extremum seeking control has also a large application, such as solar cell management, blade adjustment in water turbines and windmills to maximize the generated

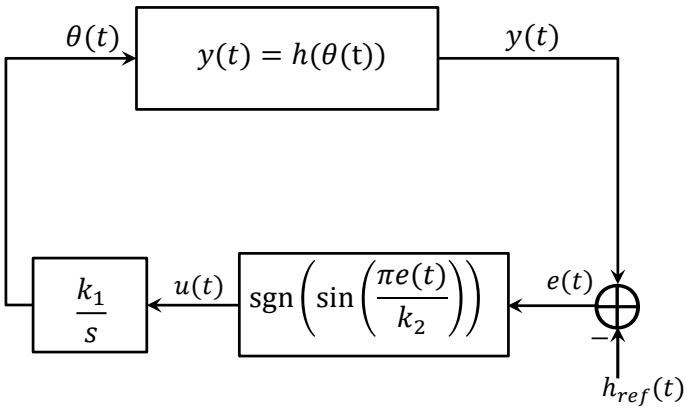

Figura 1.4: Block diagram of the sliding mode based extremum seeking

power, Anti-lock Breaking Systems (ABS), cooling systems and autonomous vehicles without position sensing, neuromuscular electrical stimulation [5, 44]. In [45] and in the 180 references therein, many real-world applications are also presented.

Multivariable Extremum Seeking Control

Many problems that require real-time optimization are naturally multivariable [5], such as in energy conversion systems for renewable energy sources [46] and air-conditioning systems [47].

The first studies of multivariable extremum seeking control were provided by Rotea [24] and Walsh [48], and their results were for plants with constant parameters and a systematic design procedure was absent [21]. Stability analysis for general multivariable ESC and systematic design guidelines for stability/performance were thereafter supplied in [49].

There are two types of multivariable ESC schemes [1, 47]:

1. Gradient-based multivariable ESC;

2. Newton-based multivariable ESC.

Gradient-based multivariable ESC is an extension of scalar gradient-based ESC described in this section, having a dither signal vector with different frequencies $S(t) = [a_1 \sin \omega_1 t \cdots a_n \sin \omega_n t]$ and demodulation signal vector $M(t) = [\frac{2}{a_1} \sin \omega_1 t \cdots \frac{2}{a_n} \sin \omega_n t]$, which extract the gradient information, as illustrated in Figure 1.5. The positive constants a_i and ω_i are the dither amplitudes and frequencies, respectively, associate with each input variable, θ is the plant input, $\hat{\theta}$ is the estimate of the optimizer, $\hat{G}$ is the estimated gradient information, $\frac{s}{s+w_h}$ and $\frac{\omega_l}{s+\omega_l}$ are high-pass and low-pass filters, respectively. By the modulation and demodulation process, the gradient $\hat{G}$ with reference to different input variables can

be estimated. The integrator is then used to drive the gradient to zero. For a convex performance map, a point with zero gradient would mean that this point is the optimum working point. This algorithm has the disadvantage of local convergence and its rate depends on the Hessian [1]. The Newton-based ESC was proposed to circumvent the latter drawback.

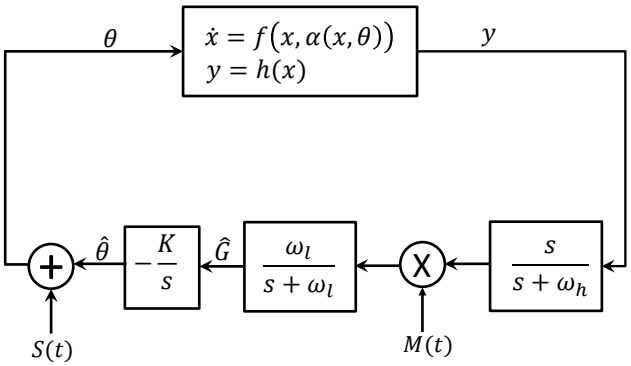

Figura 1.5: Gradient-based multivariable ESC

Figure 1.6 illustrates the Newton-based multivariable ESC algorithm, which can be divided in two parts: the demodulation matrix $N(t)$, which generates an estimate of the Hessian denoted by H, and the Riccati equation

$$\dot{\Gamma} = \omega_r \Gamma - \omega_r \Gamma \hat{H} \Gamma, \quad \omega_r > 0, \tag{1.8}$$

which generates an estimate of the inverse of the Hessian matrix H^{-1}, even when the estimate of the Hessian is singular. The key distinction of the Newton algorithm relative to the gradient algorithm is that, while the convergence of the gradient algorithm is dictated by the second derivative (Hessian) of the map, the convergence of the Newton algorithm is independent of the Hessian and can be arbitrarily assigned. This is particularly important in non-model based algorithms, like extremum seeking, where the Hessian is unknown [1]. Experimental results comparing the gradient and Newton-based methods are performed in [46], in which the authors optimize a photovoltaic array system, by tuning the duty cycles of DC/DC converters employed in the system.

Recently, a multivariable perturbation-based ESC [9] for general nonlinear dynamical plants was proposed, in which the closed-loop plant and controller is globally asymptotically stable (GAS). This result is based on the amplitude and frequencies of the perturbations being time varying and asymptotically decaying to zero as the time goes to infinity. However, one should note that this is usually not desirable, because if the perturbation vanishes, then any measurement noise is free to drive the output away from its extremum value. Moreover, it is known that this perturbation-based ESC has a drawback, the convergence rate slows down within the domain of

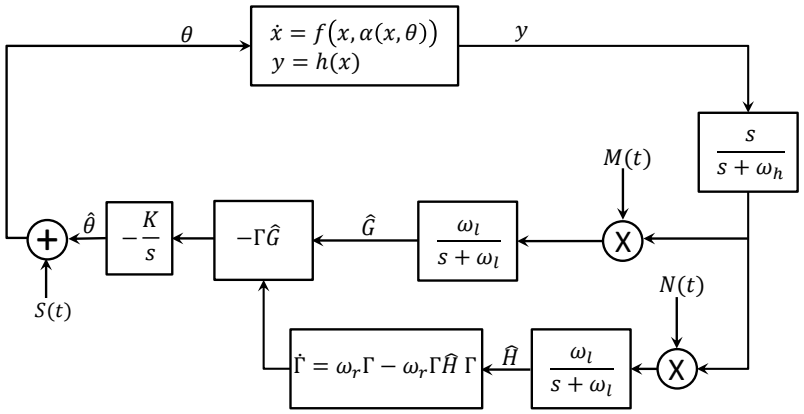

Figura 1.6: Newton-based multivariable ESC

attraction [50, 51].

In the context of sliding mode control, in [52] the authors proposed a multivariable sliding mode ESC by applying a sliding manifold vector for multivariable control. The proposed controller is compared to multivariable gradient-based method through experimental studies, registering advantages in terms of speed, accuracy and robust performance. However, their stability proof seems to be inconsistent. Earlier, Korovin and Utkin [41] suggested solving multivariable extremum seeking control through an one-dimensional network by varying the direction of the search in space, but they were not clear when the direction should be changed. Then, the authors in [53] solved this issue by using a minimum peak detector, which tracks the input signal and holds the minimum of its output from the previous reset, by using two hysteresis devices. However, for n-dimensional network, additional $2n-1$ relays and parameters would be needed, which may lead to a more complex implementation. Moreover, the oscillations around the optimizers varies according to such $2n-1$ parameters, which must be also different.

In [17] and [54], the authors also proposed an extremum seeking strategy based on sliding modes and periodic switching functions in order to address static multi-input multi-output (MIMO) maps. Both apply the control strategy to Raman optical amplifiers. The latter relaxes the condition of diagonal dominance to triangular dominance, although remain the need for a weak coupling between the input and output channels.

Recently, Salamah and Özgüner [2] proposed a sliding mode-based MESC, similarly to [41, 53], by employing a periodic switching function and a periodic search function (cyclic search), to optimize energy production in wind farms. Cyclic search means that each channel is active at a time, in such a way that while the channel is active, the others are frozen at their previous optimum values. However, the authors formulate a restrictive assumption about the directional derivatives, which cannot

be verified due to the multiple extrema in the multiparameter search.

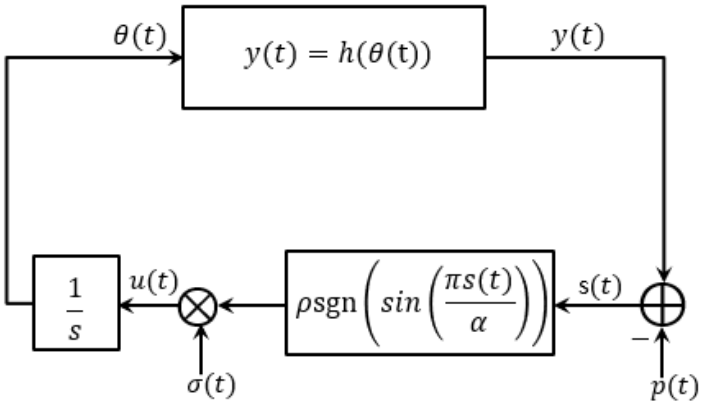

Figura 1.7: Sliding mode based multivariable ESC

Figure 1.7 illustrates the control scheme proposed in [2], where $p(t)$ is a monotonically decreasing function (for a minimization problem), $\sigma(t)$ is the periodic search function and $u(t)$ is the sliding mode control law.

We conclude this section with a summary of the theoretical results on multivariable extremum seeking control, shown in Table 1.

In such table, the references are listed in chronological order according to each approach: Gradient-based, Newton-based and Sliding mode based ESC. The third column brings the number of inputs and outputs, i.e., if the objective function is MIMO or MISO. Static/Dynamic and Linear/Nonlinear indicate the underlying process dynamics. Column Global/Local concerns to the type of stability/convergence properties.

Table 1: Summary of previous theoretical results on multivariable ESC.

Reference	ESC approach	No. I/O	Static/Dynamic map	Global/Local Convergency	Linear/Nonlinear plant
ROTEA (2000)	Gradient-based	MIMO	Static	Local	Nonlinear
WALSH (2000)	Gradient-based	MISO	Dynamic	Local	Nonlinear
ARYUR e KRSTIĆ (2002)	Gradient-based	MISO	Dynamic	Local	Nonlinear
CREABY *et al.* (2009)	Gradient-based	MISO	Dynamic	Local	Nonlinear
FRIHAUF *et al.* (2012)	Gradient-based	MIMO	Static	Local	Nonlinear
XIAO *et al.* (2014)	Gradient-based	MISO	Static	Local	Nonlinear
OLIVEIRA *et al.* (2015)	Gradient-based	MISO	Static	Local	Nonlinear
OLIVEIRA *et al.* (2017)	Gradient-based	MISO	Static	Local	Nonlinear
HARING e JOHANSEN (2017)	Gradient-Based	MISO	Dynamic	Global	Nonlinear
BAGHERI *et al.* (2018)	Gradient-based	MISO	Static	Local	Nonlinear
LIU *et al.* (2018)	Gradient-based	MISO	Dynamic	Local	Nonlinear
OLIVEIRA *et al.* (2020)	Gradient-based	MISO	Dynamic	Local	Nonlinear
GHAFFARI *et al.* (2012)	Newton-based	MISO	Static	Local	Nonlinear
OLIVEIRA *et al.* (2015)	Newton-based	MISO	Static	Local	Nonlinear
GHAFFARI *et al.* (2014)	Newton-based	MISO	Static	Local	Nonlinear
TOLOUE e MOALLEM (2017)	Sliding mode based	MISO	Static	Local	Nonlinear
SALAMAH e ÖZGUNER (2018)	Sliding mode based	MISO	Static & dynamic	Local	Nonlinear
PEIXOTO *et al.* (2020)	Sliding mode based	MIMO	Static	Global	Nonlinear
Proposed algorithms	Sliding mode based	MISO	Static & Dynamic	Global	Nonlinear

1.3 List of Publications and Contributions

The following conference papers are not part of the thesis, but served as the main background works to be extended to the proposed multivariable approaches:

- Aminde, N. O., Oliveira, T. R., Hsu, L. Global Output-Feedback Extremum Seeking Control via Monitoring Functions. In *Proceedings of the 52nd IEEE Conference on Decision and Control*, pages 1031–1036, Florence, Italy, December, 10-13, 2013.

- Oliveira, T. R., Aminde, N. O., Hsu, L. Monitoring Function based Extremum Seeking Control for Uncertain Relative Degrees with Light Source Seeking Experiments. In *Proceedings of the 53rd IEEE Conference on Decision and Control*, pages 3456–3462, Los Angeles, California, December, 15-17, 2014.

- Oliveira, T. R., Peixoto, A. J., Hsu, L. Global real-time optimization by output-feedback extremum-seeking control with sliding modes. *Journal of The Franklin Institute*, pages 1397–1415, v. 349, 2012.

The following list of publications forms the basis of this thesis, and consequently our contributions:

- Aminde, N. O., Oliveira, T. R., Hsu, L. Controle Extremal para Mapeamentos Dinâmicos Multivariáveis usando Função de Monitoração e Busca Cíclica. *XV Simpósio Brasileiro de Automação Inteligente (SBAI)*, 2021.

- Aminde, N. O., Oliveira, T. R., Hsu, L. Multivariable Extremum Seeking Control via Cyclic Search and Monitoring Function. *International Journal of Automation, Control and Signal Processing*, 2020 [61]. (CAPES Qualis A2).

- Aminde, N. O., Oliveira, T. R., Hsu, L. Controle Multivariável para Busca Extremal Cíclica Usando Modos Deslizantes e Função de Chaveamento Periódica. *Congresso Brasileiro de Automática (CBA)*, 2020.

- Aminde, N. O., Oliveira, T. R., Hsu, L. Controle Extremal Cíclico Multivariável via Função de Monitoração. *XIV Simpósio Brasileiro de Automação Inteligente (SBAI)*, 2019.

These contributions can be summarized in two branches, subdivided in three main topics:

- Multivariable sliding mode based ESC algorithms for static maps;

  (1) Monitoring function-based with cyclic search. Published in [61] and described in chapter 2.

  (2) Periodic switching function-based with cyclic search. Presented at CBA 2020, described in chapter 3 and to be submitted to a Journal.

- Multivariable sliding mode based ESC algorithms for dynamic maps with arbitrary relative degree;

  (1) Presented at SBAI 2021, described in chapter 4 and indicated by the conference committee to be published at Journal of Control, Automation and Electrical Systems (JCAE). This treats the systems with arbitrary relative degree, relying on a time-scale separation between the process dynamics and the extremum seeking controller dynamics.

1.4 Overview of the Thesis

The contents of this thesis are as follows.

Chapter 2 presents specifically the design and analysis of multivariable extremum seeking controller for static maps via monitoring function and cyclic search

Chapter 3 presents the design of the multivariable extremum seeking controller for static maps via periodic switching function.

Chapter 4 presents the design and analysis of the multivariable extremum seeking control applied for dynamic maps with arbitrary relative degree.

Chapter 5 summarizes and concludes the thesis.

Capítulo 2

Multivariable Extremum Seeking Control via Monitoring Function and Cyclic Search Directional

In this chapter, we extend our results from [13] to a multivariable approach, i.e., we propose a novel multivariable extremum seeking based on cyclic search direction and monitoring function for sliding-mode tracking with unknown control direction. The cyclic search was inspired from the periodic search function proposed in [2], which basically considers the multivariable problem as a sequence of scalar sub-problems. The latter was based on sliding-mode generated by periodic switching functions. Unlike earlier publications [1, 2, 52], where just local convergence could be assured, global convergence properties of the search algorithm are now guaranteed. Moreover, when compared to the semi-global scheme proposed in [50, 62], our results have one more advantage, since the rate of convergence does not slow down within the global domain of attraction. The following section is a substantial transcription of a published paper at the International Journal of Automation, Control and Signal Processing, available here.

Notation and Terminology - Throughout this chapter, the Euclidean norm of a vector x and the corresponding induced norm of a matrix A are denoted by $\|x\|$ and $\|A\|$, respectively. From a technical standpoint, the theoretical results obtained in this chapter are based on Filippov's definition for solution of differential equations with discontinuous right-hand sides [63]. As in [14, 64], a generic vector function $f(t)$ is said to be of order $\mathcal{O}(\mu)$ over an interval $[t_1, t_2]$ if there exists positive constants κ and, μ^* such that, $\|f(t)\| \leq \kappa\mu$, $\forall \mu \in (0, \mu^*]$ and $\forall t \in [t_1, t_2]$. For the sake of simplicity, throughout the chapter, we will not give estimates of constants κ and μ^* and thus will not quantify a corresponding $\mathcal{O}(\mu)$ approximations. On the other hand, we will be satisfied by $\mathcal{O}(\mu)$ being an "order of magnitude relation", valid for "μ

sufficiently small" so that it can be made arbitrarily small. This is our quantitative characterization of "small neighborhood".

2.1 Problem Statement

Consider a nonlinear multivariable map $h : \mathbb{R}^n \to \mathbb{R}$ given by

$$y = h(x), \tag{2.1}$$

where $x \in \mathbb{R}^n$ and $y \in \mathbb{R}$. The objective is to find the extremum (maximum) point $x^* \in \mathbb{R}^n$, that maximizes y, as close as possible.

This problem can be recast into the context of ESC by introducing the system,

$$\dot{x} = u, \tag{2.2}$$
$$y = h(x), \tag{2.3}$$

with the control input given by a vector $u \in \mathbb{R}^n$, which is to be designed so that the extremum seeking objective is accomplished.

With respect to the controlled plant, the following assumptions are made:

(A1) (*Differentiability of h*): The function $h : \mathbb{R}^n \to \mathbb{R}$ is continuously differentiable over all domain $\mathbb{R}^n$.

Let the gradient and Hessian matrices of $h(.)$ be defined as

$$\frac{\partial h}{\partial x} = \left[\frac{\partial h}{\partial x_1} \quad \cdots \quad \frac{\partial h}{\partial x_n}\right]^T \text{ and } \left[\frac{\partial^2 h}{\partial x^2}\right]_{ij} = \frac{\partial^2 h(x)}{\partial x_i \partial x_j}, \quad i, j = 1, \ldots, n.$$

(A2) (*Unique maximum of h*):

Assume that there exists $x^* \in \mathbb{R}^n$ such that $y^* = h(x^*)$ is the unique maximum of $h(x)$, where the gradient and the Hessian matrices satisfy, respectively:

$$\left.\frac{\partial h}{\partial x}\right|_{x=x^*} = 0 \text{ and } \left.\frac{\partial^2 h}{\partial x^2}\right|_{x=x^*} < 0,$$

where $x \in \mathbb{R}^n$.

(A3) (*Radial unboundedness of h*): The function $h : \mathbb{R}^n \to \mathbb{R}$ is assumed radially unbounded in $\mathbb{R}^n$. This guarantees that if $|y|$ is bounded, then $\|x\|$ must be bounded.

The mapping h as well as its gradient are considered unknown to the control designer. We wish to find an output-feedback control law u such that, from any initial condition, the system is steered to remain in an arbitrarily close vicinity of the extremum point y^*. Without loss of generality, we only address the maximum seeking problem.

It should be noted that more general systems can be considered [13], in which x would be the state of a control system with more complex dynamics than that of simple integrators. The objective of considering the simpler system (2.2)-(2.3) is to focus on the basic ideas of an ESC method for dynamic systems with objective function depending on several inputs.

The ESC problem can be formulated as an output feedback tracking problem with unknown control direction, as explained hereafter. From (2.2) and (2.3), the first time derivative of the output y is given by

$$\dot{y} = \frac{\partial h}{\partial x}^T u, \tag{2.4}$$

where the plant high-frequency gain (HFG), denoted by k_p, is given by the gradient vector, i.e.,

$$k_p(x) := [k_{p_1} \quad \cdots \quad k_{p_n}], \tag{2.5}$$

$$k_{p_i}(x) := \frac{\partial h}{\partial x_i}. \tag{2.6}$$

As in [14], the signs of the elements of k_p can be seen as *control directions*. The assumption (**A2**) leads us to consider a nonlinear control system with a state dependent HFG, with respect to each control component u_i, which may change sign with time, around the extremum or optimum point of interest.

2.2 Multivariable Controller via Cyclic Search and Monitoring Function

The proposed output-feedback multivariable ESC based on a cyclic search and monitoring function scheme is illustrated in Figure 2.1. The control law for plants with unknown HFG is defined as in [13]:

$$u(t) = \begin{cases} u(t)^+ &= -\rho(t)\sigma(t)\,\mathrm{sgn}(e(t))\,, \ t \in T^+\,, \\ u(t)^- &= \rho(t)\sigma(t)\,\mathrm{sgn}(e(t))\,, \ t \in T^-\,, \end{cases} \tag{2.7}$$

where, the tracking error e is defined as

$$e(t) = y(t) - r(t)\,, \tag{2.8}$$

and $r(t)$ is a simple ramp time-function generated by the reference model

$$\dot{r}(t) = p, \quad r(0) = y(0)\,, \tag{2.9}$$

where $p > 0$ is a design constant. Optionally, and for the sake of practical consistency, such ramp can be saturated at a high enough value. In the control law (2.7), $\rho(t)$ is a positive scalar modulation function (or gain) to be designed in section 2.4, and $\sigma(t)$ is a cyclic *vector* search function which alternates periodically the search direction, to be defined in section 2.3.

In Figure 2.1, the search directions correspond to each of the state variable axes, without loss of generality. The sets T^+ and T^- satisfy $T^+ \cap T^- = \emptyset$ and $T^+ \cup T^- = [0, t_M)$. Here, t_M is the maximal time of existence of a solution for the closed-loop system, i.e., t_M is finite if the system escapes in finite-time or infinite otherwise. Our design for the ESC system will guarantee bounded system signals and convergence to the extremum point. Thus, it will be proved that no finite-time escape may occur, so that $t_M = \infty$.

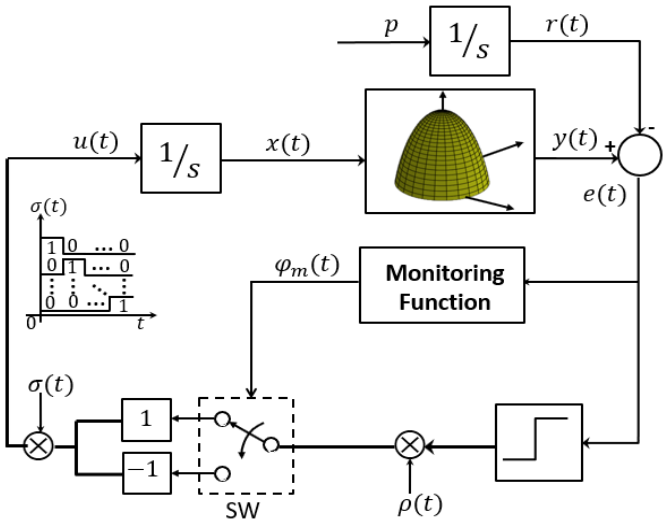

Figura 2.1: Block diagram of the proposed multivariable ESC via cyclic search. A monitoring function governs the sign switching (SW) of the output tracking sliding mode control.

The idea behind using a ramp as reference model and sliding mode control (SMC) for synthesizing the control signals is simple (see [65]). SMC is known for its capability of performing precise tracking under uncertainty. Suppose that the optimal point is a maximum. Then, an increasing ramp ($p > 0$) is chosen and is to be tracked by the objective function. This forces it to grow up to reach its maximum value. To avoid bad transients, the reference ramp can start at the initial output value $y(0)$ at $t = 0$. Then, perfect sliding mode (SM) tracking can be achieved from the very

beginning of the extremum seeking process or after a short transient.

Obviously, for the case of minimum seeking, a decreasing ramp should be chosen ($p < 0$). The modulation function $\rho(t)$ in (2.7) is designed so that $y(t)$ tracks $r(t)$ as long as possible. In this way, $y(t)$ is forced to achieve the vicinity of the maximum $y^* = h(x^*)$ and to remain close to the value y^*, i.e, x close to the maximizer point x^*.

This behavior is simpler to understand in the scalar ESC problem. As explained in [13], the "hill climbing" sliding mode starts, possibly after a short time interval taken to identify the correct control gain sign by the monitoring function, until the control gain becomes exceedingly reduced, tending to zero close to the extremum point. Then, "controllability" is lost within some small Δ-vicinity of the extremum point, as introduced later in Assumption **(A4)**. Inside this vicinity, the modulation function will not be large enough to maintain the sliding mode. However, the control law will maintain y close to the optimal value y^*.

In the multivariable case, the scenario is more complicated. Even reducing the problem to piece-wise scalar problems by means of the cyclic search strategy, in every search direction, extremum points different from the global one generally exist. These will be referred as "directional maximum or extremum". Even so, it will be shown that the global maximum will be ultimately attained by the proposed cyclic search strategy.

Remark 1 *The paper [2] adopts the cyclic search followed in our work. However, it makes a quite restrictive assumption about the ith directional derivative in that it must be nonzero when the ith control parameter θ_i is not equal to its value (θ_i^*) at the unique extremum of the objective function (see Assumption 2.1). Their assumption is not satisfied even for a quadratic objective function. In our method, such assumption is not made. This is why, along a directional search, extremum points can exist and yet convergence to the global maximum can be guaranteed.*

2.3 Design of the Cyclic Search Direction

The cyclic directional search is designed so that the change of the search direction takes place periodically. Let $\sigma(t)$ be a periodic function with period T_s, i.e., $\sigma(t + T_s) = \sigma(t)$ (see detail in Figure 2.1). Let the interval $\mathcal{T} = [\mathcal{T}_l, \mathcal{T}_u)$ (open right-side to avoid ambiguities) represent the interval of one cycle so that $T_s = \mathcal{T}_u - \mathcal{T}_l$ and let the set of initial instants of each directional search be denoted as $\tau_1, \tau_2, \cdots, \tau_n$. By convention, let $\mathcal{T}_l = \tau_1 < \tau_2 < \cdots \tau_n < \tau_{n+1} = \mathcal{T}_u$, and let $\Delta\tau_i = [\tau_i, \tau_{i+1}), \forall i = 1, ..., n$, be the n directional search sub-intervals within each cycle. Let the orthonormal basis be denoted by $a_1, a_2, \cdots, a_n \in \mathbb{R}^n$, so that

$a_i^T = [0, \cdots 0, 1, 0 \cdots 0]$, with the unit element at ith position of the vector. Thus, the cyclic search direction in (2.7) can be defined as follows:

$$\sigma(t) = a_i, \quad \forall t \in \Delta\tau_i, \quad \forall i = 1, ..., n, \tag{2.10}$$

For simplicity, we choose the duration of each sub-interval $\Delta\tau_i$, equally distributed, i.e., given by $\frac{T_s}{n}$. Therefore, during each sub-interval, the controller will search in the ith direction before switching to the next direction [2] in the next sub-interval, i.e., the multivariable controller works as a scalar controller in each sub-interval $\Delta\tau_i$. Since the search is cyclic with period T_s, to each cycle is attributed an index $\kappa = 1, 2, \ldots, \infty$. For the κth cycle, a directional extremum can occur for each ith search direction within the cycle. Such extremum is denoted $y_i^*(\kappa)$ $(= h(x_i^*(\kappa))$, where $x_i^*(\kappa) \in \mathbb{R}^n$ is an extremum point along the ith search of the κth cycle. When the system approaches the global extremum or some directional extremum, the controllability is "lost"in the sense that the control gains become too low to ensure the desired output tracking by sliding mode. Thus, the following assumption and concepts are introduced.

(A4) (*Low controllability regions* $\mathcal{D}_\Delta$ *and* $\mathcal{D}(\kappa)_{\Delta_i}$):

Let $\mathcal{D}_\Delta := \{x : \|x - x^*\| < \Delta/2\}$ and, for each ith directional search of the κth cycle, indexed κ, $\mathcal{D}(\kappa)_{\Delta_i} := \{x : \|x_i(\kappa) - x_i^*(\kappa)\| < \Delta_i/2, \quad x_j(\kappa) = \text{constant}, \ j \neq i\}$. Both regions will be referred to as Δ-vicinity, for simplicity.

Then, assume that there exists a class $\mathcal{K}$ function $L_h(.)$ such that, for any given constants $\Delta > 0$ and $\Delta_i > 0$,

$$L_h(\Delta) \leq \left\| \frac{\partial h}{\partial x} \right\|, \ \forall x \notin \mathcal{D}_\Delta, \ \text{ and } \ L_h(\Delta_i) \leq \left| \frac{\partial h}{\partial x_i} \right|, \ \forall x_i \notin \mathcal{D}(\kappa)_{\Delta_i}.$$

From the continuity assumption (A1), $L_h(\Delta)$ and $L_h(\Delta_i)$ tend to zero as Δ and Δ_i tend to zero. Note that Δ can be chosen arbitrarily small as L_h is allowed to be small enough, due to assumption (A1). For simplicity, one can choose $\Delta = \Delta_i$. Moreover, from (2.5) and (A1), k_p $(\forall x \notin \mathcal{D}_\Delta)$, and k_{p_i} $(\forall x \notin \mathcal{D}(\kappa)_{\Delta_i})$ satisfy

$$0 < \underline{k}_p \leq \|k_p\|, \|k_{p_i}\|; \tag{2.11}$$

where the lower bound $\underline{k}_p \leq L_h$ is a constant.

It is convenient to relate the parameter Δ or Δ_i with a small parameter μ, to be defined in section 2.5, in such a way that $|x - x^*| < \mu$ in $\mathcal{D}_\Delta$ and $|x_i(\kappa) - x_i^*(\kappa)| \leq \mu$ in the ith directional domain $\mathcal{D}(\kappa)_{\Delta_i}$.

In what follows, we drop the periodic search cycle index κ to avoid clutter, assuming that the analysis takes place within a generic cycle.

2.4 Error Dynamics

From (2.3), (2.8) and (2.9), by adding and subtracting λe, the time derivative of error e (hiding t) one has:

$$\dot{e} = \sum_{i=1}^{n} \frac{\partial h}{\partial x_i} u_i - p + \lambda e - \lambda e \,, \tag{2.12}$$

and for the ith search direction,

$$\dot{e} = -\lambda e + k_{p_i}(x)(u_i + d_e) \,, \tag{2.13}$$

where $\lambda > 0$ is an appropriate constant and

$$d_e := (k_{p_i}(x))^{-1} \left(-p + \lambda e\right) \,. \tag{2.14}$$

Suppose that when we start at $t = \tau_i$, i.e., at the beginning of the ith sub-period, we have controllability of the error, with $k_{p_i} \geq L_h(\Delta_i)$, to be refereed as the *condition of controllability* (see (A4)). Considering d_e as a perturbation, it can be upper bounded in absolute value by:

$$\bar{d}_e := L_h^{-1} \left(p + \lambda |e|\right) \geq |d_e| \,. \tag{2.15}$$

Based on the monitoring function proposed in [66, 67], one can rewrite the control law (2.7) for the ith search direction on the system (2.2)–(2.3) yielding the following sliding-mode control law

$$u_i = -\rho U(t) \operatorname{sgn}(e) \,, \quad u_j = 0 \,, \quad \forall j \neq i \,, \quad \text{and} \quad i \,, j \in \{1, \ldots, n\} \,, \tag{2.16}$$

where the modulation function ρ is given by

$$\rho = \bar{d}_e + \gamma, \tag{2.17}$$

with $\gamma > 0$ being an arbitrary design positive constant, and $U(t) = +1$ or -1, according to the estimated sign of k_{p_i}. If correctly estimated, $U = \operatorname{sign}(k_{p_i})$, otherwise $U = -\operatorname{sign}(k_{p_i})$. In the control diagram illustrated in Figure 2.1, U corresponds to the position of the switching key SW.

In order to guarantee the existence and uniqueness of the solutions of (2.2)–(2.3), the control law should be designed so that the closed loop system satisfies the local Lipschitz condition required in Filippov's theory on each side of a sliding surface. This is indeed the case for the feedback law (2.16), provided $k_{p_i}(x)$ is locally Lipschitz continuous and this is guaranteed by assumption (A1). Although finite-time escape

is not precluded, it will be shown in Proposition 1 that this does not occur.

In the following section, we design a monitoring function to estimate the correct sign of k_{p_i} and thus assign the value $+1$ or -1 to U.

2.5 Monitoring Function Design

The monitoring function was introduced and developed in [66, 67] and it was originally applied to scalar ESC in [13]. Basically, it is constructed by applying the Comparison Theorem [63, Theorem 7] to (2.13) which satisfies $\dot{e} \leq -\lambda e$, if the sign of k_{p_i} is correctly estimated and the control law (2.16) is applied. Thus, the solution of the following first-order differential equation:

$$\dot{\zeta} = -\lambda\zeta, \quad \forall t \geq \tau_1, \quad \zeta(\tau_1) = e(\tau_1), \tag{2.18}$$

where τ_1 denotes the initial time for (2.18), satisfies

$$|e(t)| \leq |\zeta(t)|, \quad \zeta(t) := |e(\tau_1)|e^{-\lambda(t-\tau_1)}, \ \forall t \geq \tau_1. \tag{2.19}$$

Noting that (2.19) holds when the control direction is correct, it seems natural to use ζ as a benchmark to decide whether a switching of u in (2.7) occurs from u^+ to u^- (or vice-versa), i.e., the switching occurs only when (2.19) is violated.

A simple modification in terms of $\zeta(t)$ is made to guarantee that the monitoring function always upperbounds the tracking error, even in case of starting with wrong control direction, given by U. Consider the following function for the ith search direction,

$$\varphi_{k,i}(t) = |e(t_{k,i})|e^{-\lambda(t-t_{k,i})} + \mu, \qquad k \in \mathbb{N}_{>0}, \tag{2.20}$$

where $t_{1,i} = \tau_i$ (beginning of sub-interval) and $t_{k,i}$, for $k > 1$, are the switching times of monitoring function, $\mu > 0$ is arbitrarily small. These switching occur when the monitoring function meets the error norm and consequently a change of the control direction occurs.

Note that from (2.19) and (2.20), one has $|e(t)| < |\varphi_{k,i}(t)|$ at $t = t_{k,i}$, defined as the time instant that the monitoring function $\varphi_{mi}(t)$ meets $|e(t)|$, i.e.,

$$t_{k+1,i} := \begin{cases} \min\{t > t_{k,i} : |e(t)| = \varphi_{k,i}(t)\}, & \text{if exists}, \\ t_M, & \text{otherwise}. \end{cases} \tag{2.21}$$

Multiple switchings may occur when the directional controllability is lost, i.e., when x enters $\mathcal{D}(\kappa)_{\Delta_i}$ so that $k_{p_i} \leq L_h(\Delta)$. Then, recurrent crossings of a directional

extremum imply in changes of the control direction which can be detected by the monitoring function defined, $\forall t$, as follows,

$$\varphi_m(t) := \varphi_{k,i}(t), \quad \forall t \in [t_{k,i}, t_{k+1,i}), \quad \forall i = 1, ..., n, \quad k \in \mathbb{N}_{>0}. \tag{2.22}$$

The following inequality comes from (2.22):

$$|e(t)| \leq \varphi_m(t), \quad \forall t \in [0, t_M)\,, \tag{2.23}$$

where $\varphi_m(t)$ is the monitoring function generated by the concatenation of the exponential functions (2.20).

Figure 2.2 illustrates the tracking error norm $|e(t)|$ as well as the monitoring function $\varphi_m(t)$. Basically, at each switching time occurs a small jump with amplitude μ. This parameter determines the order of the residual variation's magnitude with respect to x^*, as will be demonstrated later on. Moreover, theoretically, μ can be arbitrary small, however, real systems always have noise and μ should overcome the measured noise.

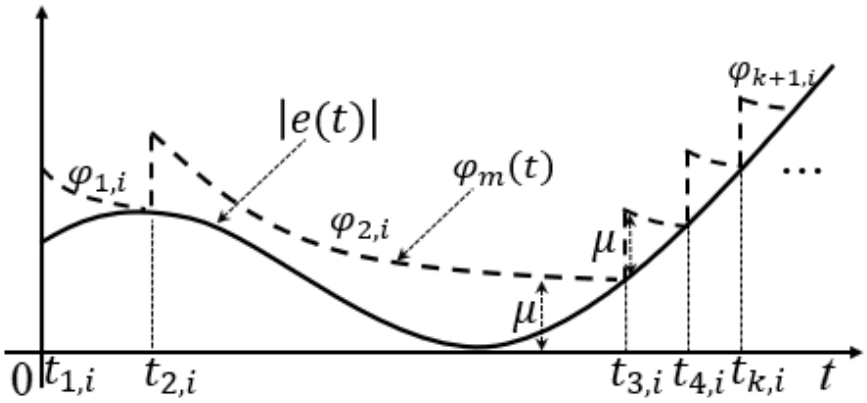

Figura 2.2: The trajectories of the monitoring function $\varphi_m(t)$ and error norm $|e(t)|$, illustrating the switching time defined by (2.21) during the ith directional search.

2.6 Dynamic Properties of Control System

The following proposition provides conditions for finding the correct control direction during any ith search direction. It guarantees that the objective function either grows or enters into a small neighborhood of some directional extremum x_i^* along the ith search direction. Moreover, finite-time escape is precluded.

Proposition 1 *Consider the system (2.2)–(2.3), reference model (2.9), search direction (2.10), control law (2.16), modulation function (2.17) and monitoring function (2.20). Consider any arbitrary initial control direction outside of regions $\mathcal{D}_\Delta$ and $\mathcal{D}_{\Delta_i}$. Then, with the ith directional search being active, one can choose $\gamma > 0$ in (2.17) sufficiently large such that* ***(a)*** *the correct control direction is reached before the time instant $\tau_i + \epsilon$, where $\tau_i > 0$ is the beginning of the ith search direction, $\epsilon > 0$ is sufficiently small and less than the sub-interval T_s/n;* ***(b)*** *the objective function $h(x)$ either increases or remains constant, modulo small oscillations, initially of order $\mathcal{O}(\mu)$ and ultimately of order $\mathcal{O}(\mu^2)$ around a ith directional extremum; in $\mathcal{D}_\Delta$ the oscillations remain of order $\mathcal{O}(\mu^2)$ after some finite time;* ***(c)*** *no finite-time escape occurs in the closed-loop system.*

Proof. The properties stated are now demonstrated.

(a) The correct control direction is reached before the time instant $\tau_i + \epsilon$, where $\tau_i > 0$ is the beginning of the ith search direction, $\epsilon > 0$ is sufficiently small and less than the sub-interval T_s/n:

If the estimated control sign is incorrect at the beginning of ith search direction, then $U = -\operatorname{sgn}(k_{p_i})$, which yields from (2.13) and (2.14):

$$\dot{e} = +|k_{p_i}|\rho \operatorname{sgn}(e) - p\,. \tag{2.24}$$

Multiplying both sides by $\operatorname{sgn}(e)$, one has for $e \neq 0$:

$$\frac{d|e|}{dt} = +\rho|k_{p_i}| - p\operatorname{sgn}(e)\,, \tag{2.25}$$

which implies that $|e(t)|$ increases, since the right-hand-side of (2.25) is positive. The monitoring function starts at $|e(\tau_i)| + \mu$ and decreases exponentially tending to μ or remains constant at μ, if $|e(\tau_i)| = 0$. Since from (2.15),(2.17) and (2.25), the growth rate of $|e(t)|$ is lower bounded by γ, it can be made arbitrarily large by increasing γ. Hence, the SW switch in Figure 2.1 will switch to the correct sign of k_{p_i} at time $(\tau_i + \epsilon)$ with sufficiently small $0 < \epsilon < \mu/\gamma$. Moreover, $|e(t)| \leq |e(\tau_i)| + \mu$ in the interval $t \in [\tau_i, \tau_i + \epsilon]$.

(b) The objective function $h(x)$ either increases or remains constant, *modulo* small oscillations around some directional extremum:

Consider the control law (2.16)–(2.17). If the control direction estimate is wrong at the start of the ith directional search ($t = \tau_i$), it is corrected shortly after according to property **(a)**. After the control direction is correctly estimated (which can occur from the starting time $t = \tau_i$), one has $U = \operatorname{sgn}(k_{p_i})$ and from (2.13), multiplying

both sides by e, one gets

$$e\dot{e} = -\lambda e^2 + |k_{p_i}|(-\rho|e| + d_e e) \tag{2.26}$$

which results from (2.17) in

$$\frac{d(e^2)}{dt} \leq -\lambda e^2 - |k_{p_i}||e|\gamma, \tag{2.27}$$

As usual, we conclude that, while the error is controllable, the proposed control law forces the tracking error to decrease and reach the sliding mode $e(t) \equiv 0$, after some finite time interval $\gamma t_{ri} = (|e(\tau_i)| + \mu)/\gamma$, arbitrarily small by increasing γ in (2.17), resulting in the increase of the objective function $h(x)$ after the sliding mode is reached. Thus, one of the following possibilities occur:

- $y = h(x)$ reaches a sliding mode and increases until the end of ith search direction, tracking the reference signal exactly.
- In sliding mode, $y(t)$ reaches the neighborhood of a directional extremum (maximum), before the end of the ith directional search loosing controllability. Then, similar to what happens in the scalar approach [14, Appendix C (ii)], [13, Appendix], the output $y(t)$ oscillates with small amplitude, initially of order $\mathcal{O}(\mu)$ and ultimately of order $\mathcal{O}(\mu^2)$ around the directional extremum (not necessarily unique) until the control switches to a new search direction (see proof of Theorem 1, item (ii)).
- If at the beginning of the ith search, the error is not controllable (in the vicinity of some directional maximum), $(y(t))$ remains inside a small interval of order $\mathcal{O}(\mu)$ and ultimately of order $\mathcal{O}(\mu^2)$, as in the previous case. In the vicinity of $\mathcal{D}_\Delta$ similar behavior of $y(t)$ holds, where the residual interval is of order $\mathcal{O}(\mu^2)$, $\forall t$ after some finite time.

The detailed analysis of oscillations around the directional extrema is made in the Proof of Theorem 1, item (ii). Thus, in any of the above possibilities, the objective function either increases or remains practically constant during the ith search direction.

(c) No finite-time escape occurs in the closed loop system:

This is a simple consequence of properties (a) and (b) since $y(t)$, and thus $x(t)$, are bounded for all t. ■

2.7 Global Convergence

In this section, the main result of the proposed output feedback multivariable controller based on a cyclic monitoring function is presented. The control algorithm drives $x(t)$ to the Δ-vicinity of the unknown x^* defined in assumption (A4). After reaching the vicinity of the maximum y^*, the objective function $y(t)$ remains around y^*, ultimately with variations of order $\mathcal{O}(\mu^2)$.

Theorem 1 *Consider the system (2.2)–(2.3), control law (2.7), reference model (2.9), search direction (2.10), modulation function (2.17) and monitoring function (2.20)–(2.22). Assume that assumptions (A1)-(A4) hold and T_s is sufficiently large. Then the region $\mathcal{D}_\Delta$ in (A4) **(i)** is globally attractive, being reached in finite time and **(ii)** once it is reached, the oscillations around y^* can be made of order $\mathcal{O}(\mu^2)$ after some finite time by choosing Δ sufficiently small.*

Proof. Outside the Δ-vicinity, the gradient of the cost function $h(x)$ does not vanish, i.e, $\left\|\dfrac{\partial h}{\partial x}\right\| \neq 0\,, \forall x \notin \mathcal{D}_\Delta$. Thus, from (2.11), $\|\underline{k}_p\|$ can be obtained from the lower bound L_h defined in (A4) which is valid globally. Furthermore, from Proposition 1, no finite-time escape occurs for the system signals.

Now, we proceed to the proof of the properties **(i)** and **(ii)** of Theorem 1.

(i) Attractiveness of $\mathcal{D}_\Delta$

The proof is made by contradiction. According to Proposition 1, for each search direction, the objective function either increases or remains ultimately constant, modulo oscillations of order $\mathcal{O}(\mu)$ or $\mathcal{O}(\mu^2)$. Thus, starting from outside the domain $\mathcal{D}_\Delta$, by property (b) of Proposition 1, the objective function y can be written as

$$y(t) = \underline{y}(t) + \tilde{y}(t)$$

where $\underline{y}(t)$ is continuous, upper bounded and nondecreasing and $\tilde{y}(t)$ is small of order $\mathcal{O}(\mu)$ or $\mathcal{O}(\mu^2)$. Thus, $\underline{y}(t)$ must tend to some constant as $t \to \infty$. Assume that this constant corresponds to a point outside the domain $\mathcal{D}_\Delta$. Then, the cyclic search will eventually pass by a search direction where the controllability holds. Then, property (b) of Proposition 1 holds for at least one of the search directions. Therefore, $\underline{y}(t)$ would still grow. This is a contradiction, since we have assumed that it would tend to a constant. Thus, the region $\mathcal{D}_\Delta$ in (**A4**) is globally attractive, being reached in finite time.

(ii) Order of oscillations around directional extrema and global extremum

Consider any ith directional search of the κth search cycle. Two possibilities arise, supposing that the period T_s is large enough.

1 The system starts controllable, i.e. outside the domain $\mathcal{D}_{\Delta_i}$ of some ith directional extremum x_i^* (possibly non-unique). Then, according to Proposition 1, either the ith directional search starts with the correct control direction ($U = \text{sgn}(k_{p_i})$ or the correct direction is estimated in a very short time. In any case, a sliding mode is realized and perfect ramp tracking shortly after the ith directional search starts. Thereafter, two possibilities arise:

1.1 The sliding mode persists until the end of the ith search and another directional search starts.

1.2 The sliding mode ceases at some time $t = t_{out}$ before the search direction changes by loss of controllability, i.e., the system enters some domain $\mathcal{D}_{\Delta_i}$. Then, the output y (objective function) moves away from the ramp, increasing with positive rate lower than p. This is seen by considering equation (2.13) cancelling the term in λ, i.e.,

$$\dot{e} = k_{p_i}(x)\rho U \,\text{sgn}(e) - p\,. \tag{2.28}$$

Now, note that, since sliding mode was active, $U = \text{sgn}(k_{p_i})$ unless it changes by the monitoring function. Due to the lack of controllability, the r.h.s in (2.28) is dominated by $-p$. Thus, for some $\varepsilon > 0$, $\dot{e}(t) < 0$ in $t \in (t_{out}, t_{out} + \varepsilon)$ so that $y(t)$ moves away from the ramp. However, $\dot{y}(t) > 0$ in the same time interval since the monitoring function will not change U for sufficiently small ε due to the continuity of $e(t)$ which is zero during the sliding mode and will not grow enough (in norm) to activate the monitoring function.

Since, $y(t)$ starts increasing, and since it is bounded from above (at least by the global maximum y^*) it will have to decrease after some finite time. This can happen in two ways. Either $y(t)$ attains its directional maximum and thereafter will remain below such maximum, or it will start decreasing before such maximum is attained by virtue of the monitoring function, which changes U to the opposite sign. In any case, for $t \geq t_{out}$ until the change of search direction, $e(t) < 0$. Under the latter condition, the control law reduces to $u_i(t) = \pm\rho(t)$, switching by virtue of the monitoring function only. Hence, the system dynamic equations (2.2)-(2.3) reduces to

$$\dot{x} = \rho U, \tag{2.29}$$

$$y = h(x), \tag{2.30}$$

where $U = \pm 1$ and switches by virtue of the monitoring function. To

characterize the dynamic behavior of such system, some simplifying assumptions are now made.

Note that ρ remains almost constant when the switchings are performed at some high frequency. Then, during some time-window encompassing a considerable number of U-switchings, ρ and the tracking error can be considered constant.

Now, U switches when $|e(t)| = \varphi_{k,i}(t)$ (see the definition (2.21)). Since here $e(t) < 0$, then $|e(t)| = -e$ so that the switching condition becomes $-e(t) = \varphi_{k,i}(t)$ or equivalently

$$-y(t) = \varphi_{k,i}(t) - r(t)\,. \tag{2.31}$$

This is the switching condition of U in terms of the output y. To characterize the motion regime of the system (2.29)-(2.30) interacting with the switching condition (2.31), we introduce the *Parabolic Recurrence Method* (PRM) described in what follows.

The basic idea is that close to a directional maximum y_i^*, taking place at $x_i = x_i^*$, i.e. inside the domain $\mathcal{D}_{\Delta_i}$ and invoking Taylor series development, the objective function deviation is parabolic with respect to $\tilde{x}_i := x_i - x_i^*$. Since (2.31) involves $-y(t)$, we define $\tilde{y} = y_i^* - y_i$. Then, $\tilde{y} \approx c^2\tilde{x}_i^2$ so that in the plane $(\tilde{x}_i, \tilde{y}_i)$, a *minimum* takes place at the origin.

We can geometrically visualize the motion regime as in Figure 2.3 by observing that, as u_i is a pulse width modulated square-wave signal, the state x_i is a triangular wave signal. Then, in the $\tilde{x}, \tilde{y}$ plane (here, to avoid clutter, the i index, in reference to the ith directional search, is dropped), the motion takes place on the parabola passing through the origin.

Starting from a point $P_1 = (\tilde{x}_1, \tilde{y}_1)$ and assuming that $U = +1$, the system moves to the right until it meets the monitoring function starting at $(\tilde{x}_1, \tilde{y}_1 + \mu)$ and decreasing approximately linearly with slope given by the initial slope of the exponentially decaying term of (2.20) minus the slope of the reference trajectory $r(t)$ at $P_1' = (\tilde{x}_1', \tilde{y}_1')$. Up to this time the parabola arc from P_1 to P_1' has been described from left to right and then U switches to -1 and the monitoring function restarts with a μ-jump at the point $(\tilde{x}_1', \tilde{y}_1' + \mu)$. The motion occurs similarly, but in the reverse sense, from right to left according to the indicated arrow. The parabolic arc from P_1' to $P_2 = (\tilde{x}_2, \tilde{y}_2)$ is then described.

In the time domain, Figure 2.4 depicts the motion described above in the zoomed sub-picture which illustrates the behavior of the output around a directional extremum, then different from the global one. It was obtained

from the simulation results of Section 2.8. Note that the vertical axis is $-\tilde{y}$ so that, instead of a maximum point, $-\tilde{y}$ tends to a minimum point and ultimately approaches the global minimum $\tilde{y}^* = 0$.

The equations relating the points P_1, P_1' and P_2 are given by

$$\tilde{x}_1'^2 + \beta\tilde{x}_1' - (\tilde{x}_1^2 + \beta\tilde{x}_1 + \mu') = 0 \quad (2.32)$$

$$\tilde{x}_2^2 - \beta\tilde{x}_2 - (\tilde{x}_1'^2 - \beta\tilde{x}_1'^2 + \mu') = 0 \quad (2.33)$$

where c is the constant from the quadratic approximation $\tilde{y} = c^2\tilde{x}^2$, $\mu' = \mu/c^2$, and $\beta = b/c^2$ with

$$b = \lambda e(t_k) + \dot{r}$$

with $-b$ being the linear slope of the monitoring function at the switching instants t_k minus the slope of the reference trajectory (p when not saturated and 0 when saturated). Note that the linear approximation of the exponentially decaying term in the monitoring function is good if the frequency of switchings is high.

The equations give a recurrence from some initial point $P_1 = P(k)$ to $P_2 = P(k+1)$. An equilibrium or fixed point satisfies $P(k+1) = P(k)$. This point is given by $\tilde{x}_1 = \tilde{x}_2$. This can be easily obtained with $\tilde{x}_1' = -\tilde{x}_1$. Then, trivially, $\tilde{x}_2 = \tilde{x}_1$. This fixed point for the recurrence (2.32)-(2.33) can be shown to be unique and is given simply by:

$$\tilde{x}_1^* = -\frac{\mu}{2\beta}\,. \quad (2.34)$$

This fixed point can be shown to be globally asymptotically stable (GAS) for the recurrence (mapping) determined by (2.32)-(2.33). Such recurrence can be written as:

$$\tilde{x}(k+1) = f(\tilde{x}(k))\,, \quad (2.35)$$

where f is continuous (2.34). Then, let us change the origin of the $(\tilde{x}(k), \tilde{x}(k+1))$ plane to the fixed point by defining the new variables $\chi(k+1) = \tilde{x}(k+1) - \tilde{x}^*$ and $\chi(k) = \tilde{x}(k) - \tilde{x}^*$. This leads to the recurrence:

$$\chi(k+1) = F(\chi(k))\,, \quad (2.36)$$

where $F(\chi) := f(\chi(k)+\tilde{x}^*) - \tilde{x}^*$, and the unique fixed point is $\chi^* = 0$. It is

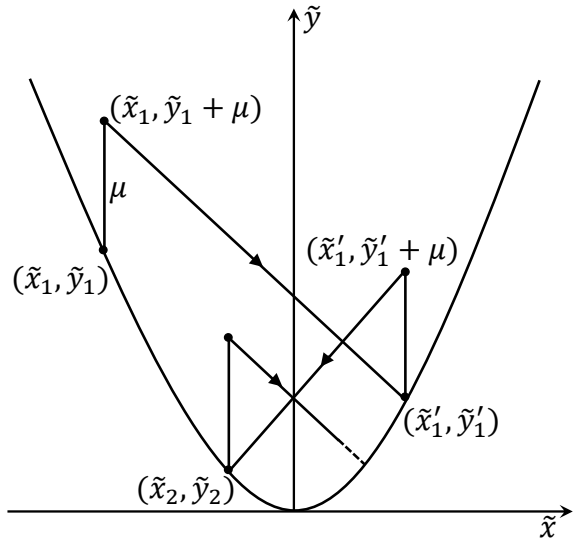

Figura 2.3: The Parabolic Recurrence Method: the starting point $P_1 = (\tilde{x}_1, \tilde{y}_1)$ is mapped to the point $P_1' = (\tilde{x}_1', \tilde{y}_1')$ and this point is mapped to $P_2 = (\tilde{x}_2, \tilde{y}_2)$. This mapping proceeds recursively. The system representative point runs the parabola forth and back, generating arcs of parabola which corresponds to the time evolution of the output $-y$ (y) close to a directional minimum (maximum).

well known that global asymptotic stability of the origin of such discrete-time system is implied if the sector condition holds [68, Lemma 3.4.1]:

$$|F(\chi)| < |\chi|, \quad \forall \chi \in \mathbb{R}, \quad \chi \neq 0. \tag{2.37}$$

The sector condition was verified to hold by plotting numerically the function F for an extensive set of parameters (β, μ') by solving (2.32) to obtain $\tilde{x}_1'$ from a given $\tilde{x}_1$ and then solving (2.33) to obtain $\tilde{x}_2$. An analytical solution is yet to be obtained.

Thus, the parabolic arcs variations are ultimately bounded by

$$|\tilde{y}| = c^2 \left(\frac{\mu}{2\beta}\right)^2 = \mathcal{O}(\mu^2).$$

Now note that, reasoning with an almost-static analysis, at the point where sliding mode ceases, the tracking error is zero so that β can be initially not so large and thus the y oscillation can be larger, according to (2.34). Since one is within a Δ-vicinity of the directional extrema when the sliding mode ceases, the oscillations will be at most of the order $\mathcal{O}(\mu)$. Moreover, since the error increases linearly, the oscillations tend asymptotically $\mathcal{O}(\mu^2)$.

2 If at the beginning of the ith search, the error is non-controllable. The situation

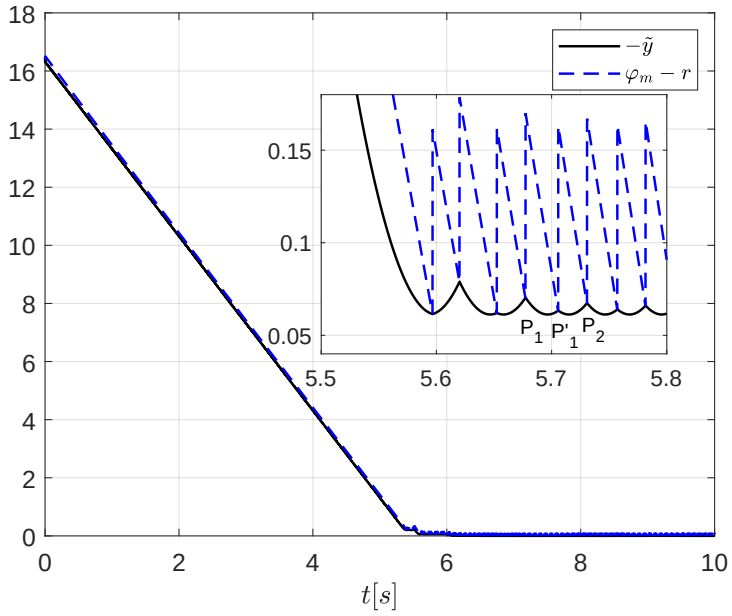

Figura 2.4: The zoomed insertion illustrates the final time window of a directional search where $-y$ converges to a neighborhood of a directional minimum, performing parabolic arcs bounded by $\mathcal{O}(\mu^2)$. The points P_1, P_1', P_2 correspond to those of Figure 2.3.

is the same as in item [1.2] above, with t_{out} coinciding with the starting time of the ith directional search.

3 Finally, if the previous case occurs within the region $\mathcal{D}_\Delta$, then $y(t) \approx y^*$ and thus, the error will grow indefinitely or up to a saturated value (more practical situation), after a finite time. Then, oscillations will remain of the order $\mathcal{O}(\mu^2)$ thereafter. ■

The extensive proof of the Theorem 1 can be summarized through the flowchart illustrated in Figure 2.5.

2.8 Illustrative Examples

As an example, consider a plant where the objective function is unknown in cascade with a simple integrator described by

$$\dot{x} = u\,, \tag{2.38}$$

$$y = -(x_1^2 + (x_2 - x_1^2)^2)\,. \tag{2.39}$$

This objective function is known as *Rosenbrock banana* function, which is used as a performance test problem for optimization algorithms [69]. Its general form

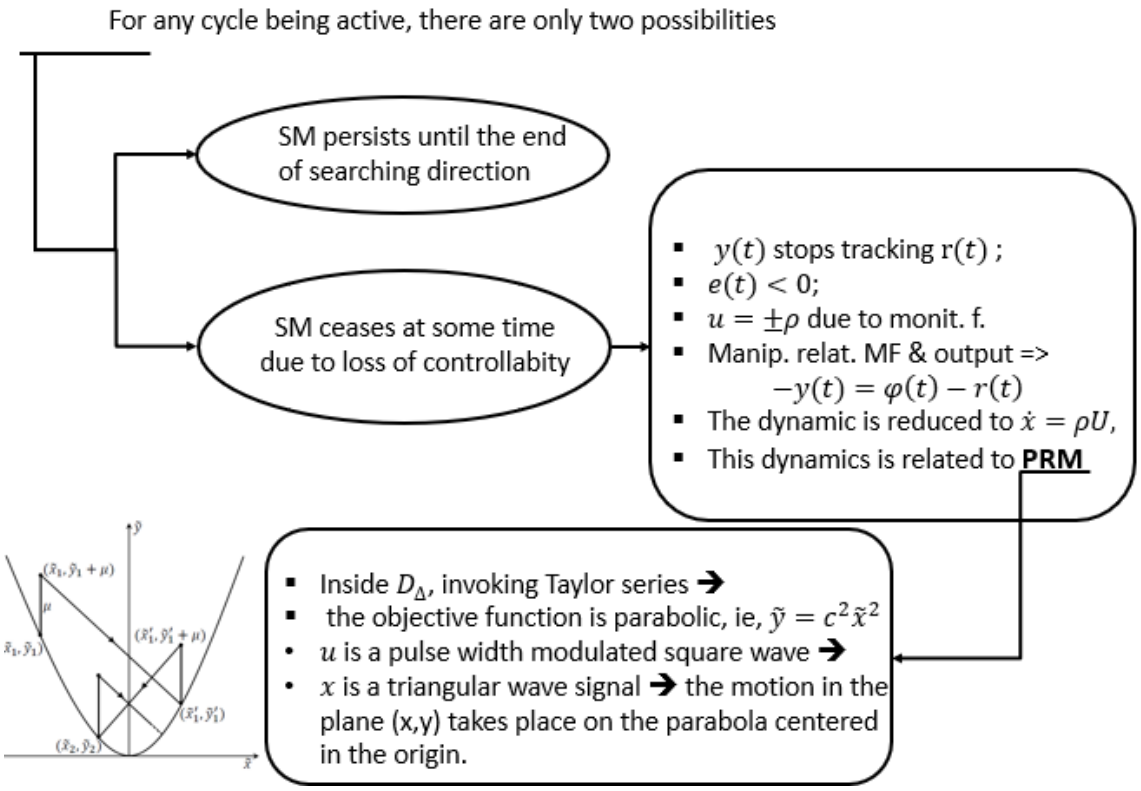

Figura 2.5: Flowchart to summarize the proof of Theorem 1. PRM means *Parabolic Recurrence Method*

is $f(x_1, x_2) = (a - x_1)^2 + b(x_2 - x_1^2)^2$, with global minimum at $(x_1, x_2) = (a, a^2)$, where $f(x_1, x_2) = 0$. In our case, we just multiplied it by -1 and considered $a = 0, b = 1$ so that the optimum parameters are $x^* = (0, 0)$ and $y^* = 0$ as illustrated in Figure 2.6. A sketch of the phase portrait (x_1 versus x_2) is shown in Figure 2.7. Note that the level surfaces illustrate that the function is non-convex. In terms of application, the objective function presented in Figure 2.6 could represent a map of power optimization of a wind turbine, where the vector x would represent torque and pitch angle [55].

The control law (2.7) can be applied with the modulation function satisfying (2.17). However, to simplify the control design we have used a constant modulation function $\rho(t) = 5$, which is adequate to reach the optimization objectives in the numerical simulations, maintaining at least local convergence results. It is reasonable to assume a constant modulation function, since we desire to have a fair comparison of our global algorithm with respect to other local existing multivariable ESC approaches found in the literature. The remaining simulation parameters were chosen according to the following values: $p = 3$, $r_0 = y(0)$, $\lambda = 1$, $T_s = 1s$ and $\mu = 0.1$.

Figure 2.8 illustrates the result of the objective control: to find the neighborhood of $x^* = (0, 0)$ and $y^* = 0$. Note that the oscillations around x^* are of order $\mathcal{O}(\mu^2)$ (see detail in Figure 2.8(b)). Figure 2.6 also shows the output signal in each search

direction, from three initial conditions, $x_0 = (-1.5, -1.5)$ (black), $x_0 = (-1.5, 1.5)$ (blue) and $x_0 = (1.5, 1.5)$ (green).

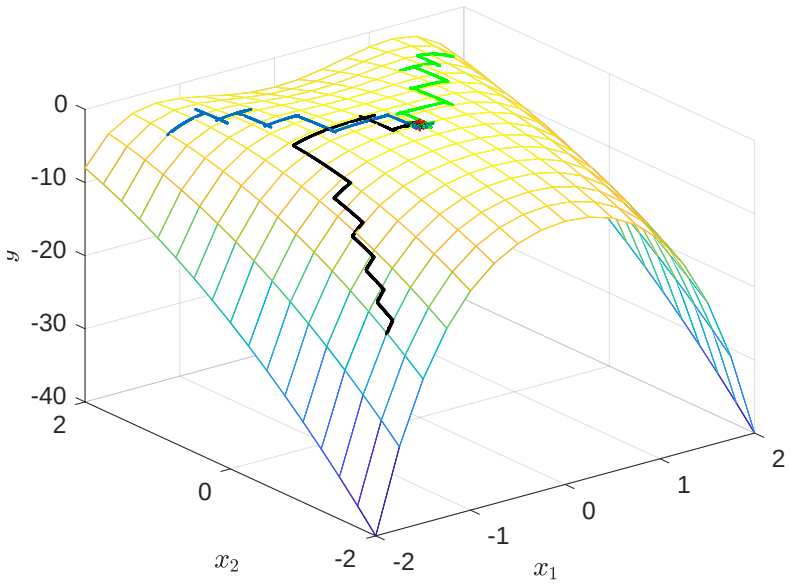

Figura 2.6: Objective function $y = h(x)$ and the convergence to the optimum value $y^* = 0$ (denoted by $*$), starting from three distinct initial conditions $x_0 = (-1.5, -1.5)$ (black), $x_0 = (-1.5, 1.5)$ (blue) and $x_0 = (1.5, 1.5)$ (green).

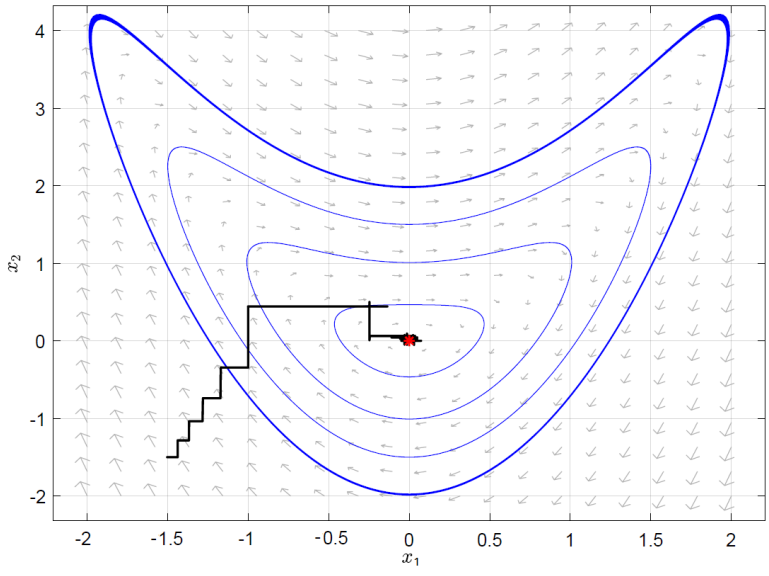

Figura 2.7: The level sets of the objective function $y = h(x)$ and the trajectory from the initial condition $x_0 = (-1.5, -1.5)$.

Figure 2.9 shows the monitoring function $\varphi_m(t)$ and the error norm $|e(t)|$. In the left zoomed part, it is clear that the simulation starts with a wrong control direction, but rapidly it switches to the correct one and then the error enters in sliding mode.

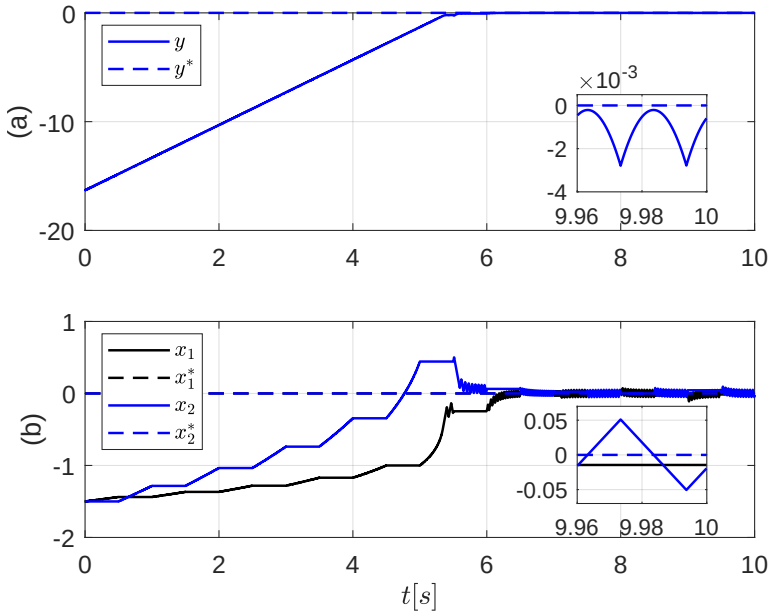

Figura 2.8: Simulation results: (a) the output of the plant converges to a small neighborhood of $y^* = 0$ and (b) the input vector x converges to a small neighborhood of $x^* = [0 \quad 0]$, with initial condition $x(0) = (-1.5, -1.5)$.

The right zoomed part shows the switching process with amplitude $\mu = 0.1$ occurring when $e(t) = \varphi_m(t)$. Such switching is caused by the lost of controllability when the directional maximum or the desired extremum is already achieved. Note that, from this moment, the error increases according to the reference trajectory with slope $p = 3$ and stops at the saturation $r(t) = 5$ (see equation (2.9)).

Both control signals u_1 and u_2 are illustrated in Figure 2.10(a) and the switching of the search direction σ_1 and σ_2 are depicted in Figure 2.10(b). In the first $0.5s$ the direction of x_1 is activated and from $0.5s$ to $1s$, in the direction of x_2. Then, the process is repeated cyclically (see Figure 2.8b). The amplitude of the control signals are defined by the modulation function, i.e, $\rho(t) = 5$. One can note the sliding-mode motion and/or high frequency switching in the control signal that could cause "*chattering*" [70]. However, it is avoided because the objective function (2.3) receives only filtered signals x from the integrator in (2.2) and (2.3). In addition, Figure 2.11 shows the output tracking of the reference trajectory accordingly to the description presented in section 2.2, i.e, the output tracks the reference until it reaches the vicinity of directional maximum or global maximum $y^* = 0$ and remains in their neighborhoods during the sub-period the loss of controllability.

On the other hand, Figure 2.12 shows the simulation result using the gradient-based multivariable ESC strategy proposed in [1]. A comparison to our results (see Figure 2.8) suggests that our approach presents an improved performance in terms of rate of convergence and faster transient, using the same initial conditions

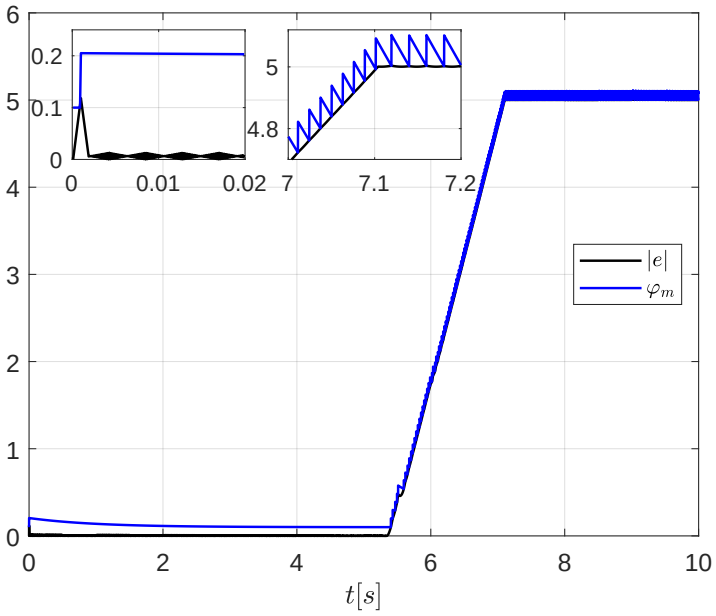

Figura 2.9: Monitoring function φ_m and error norm $|e|$. The left-side detail shows the simulation starting with incorrect control direction, the right-side detail shows the switching when (2.23) is violated.

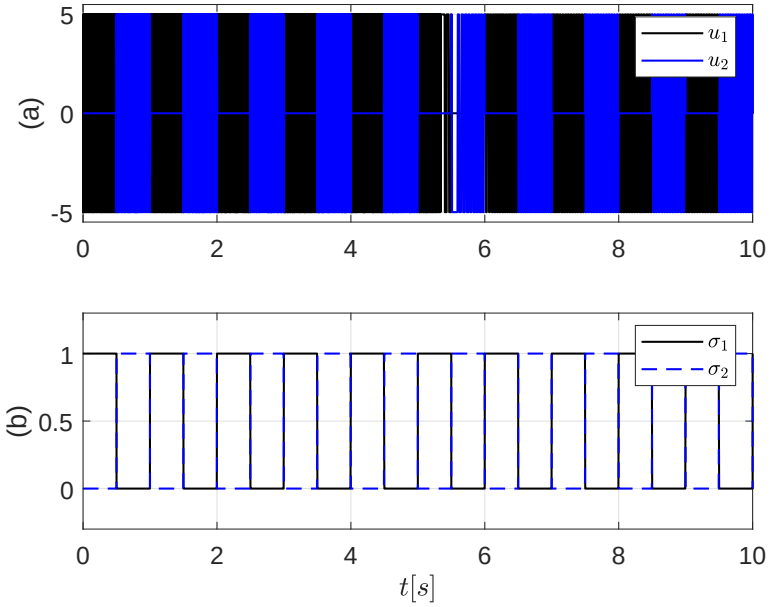

Figura 2.10: Simulation results: (a) control signals u_1 e u_2 and (b) the cyclic search direction with period $T_s = 1s$.

$x(0) = (-1.5, -1.5)$ and simulation parameters considered in [1].

The framework for the comparative simulation was built in the MATLAB R2018a/SIMULINK environment with sampling period of $t_s = 10^{-4}s$,

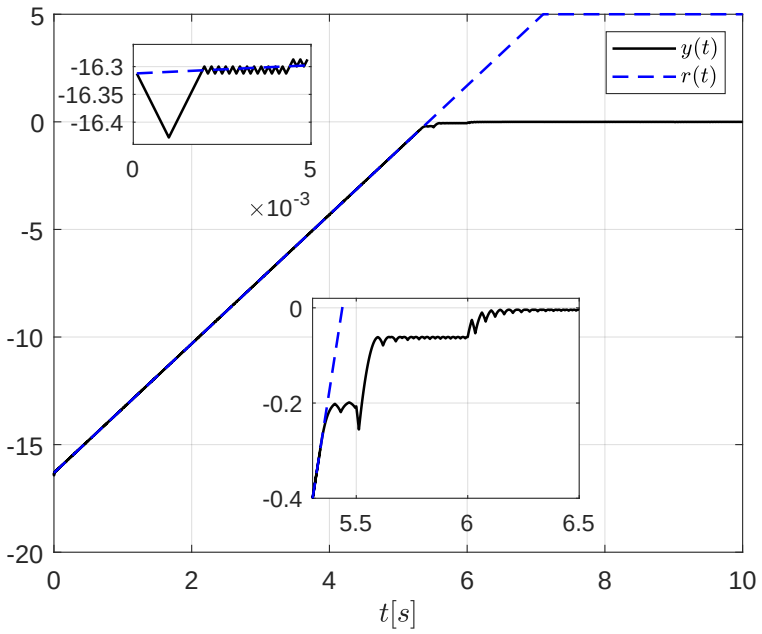

Figura 2.11: The plant output $y(t)$ tracks the reference trajectory $r(t)$ in sliding-mode until a small neighborhood of the desired maximum $y^* = 0$ is reached. Note in the zoomed sub-figure (top), the correct control direction is achieved. Other sub-figure (bottom), directional maximum is reached at each sub-period $0.5s$.

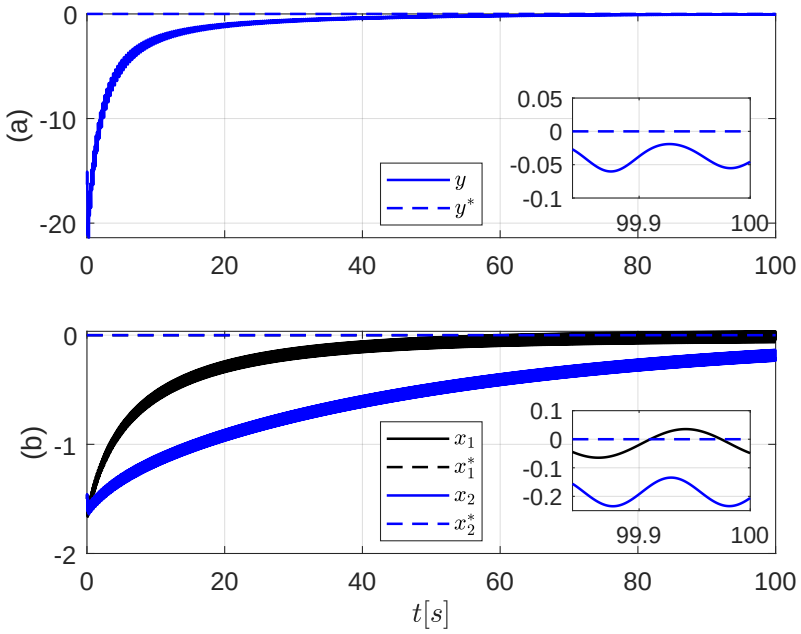

Figura 2.12: Slower responses occur when a gradient-based extremum seeking [1] is applied to the same objective function.

fixed-step and Euler solver. We also developed a Graphical User Interface (GUI) design environment, in which the user can select the number of control inputs (up

to 3), time of simulation, select the method and so on, as illustrate the Figure 2.13.

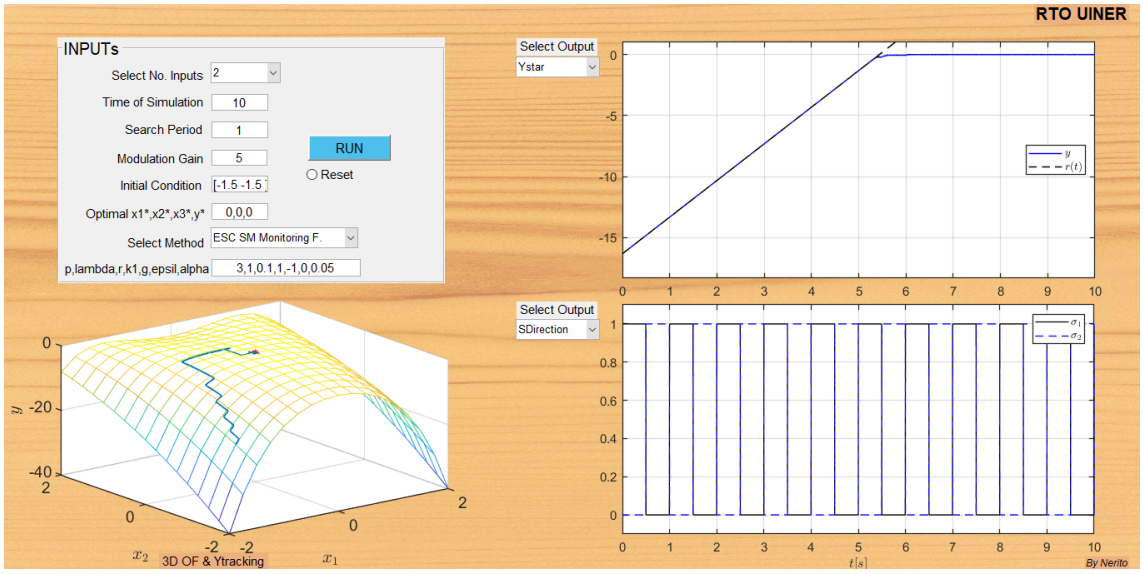

Figura 2.13: Matlab GUI used to run simulations. The GUI has communication states (input parameters) on the top left and the real time plots on the bottom left and right side.

2.9 Conclusion

A new multivariable extremum seeking control via cyclic search and monitoring function was developed for a class of uncertain nonlinear plants. The resulting approach guarantees global convergence of the system output to a small neighborhood of the extremum point. A detailed characterization of residual oscillations around the optimal point is presented based on a recurrence (point-mapping) approach denominated *Parabolic Recurrence Method*. Simulation results were carried out to illustrate the remarkable controller performance in terms of better rate of convergence when compared to an earlier proposed Newton-based method. More specific guidelines to tune the proposed algorithm are also of interest for future research.

Capítulo 3

Multivariable Sliding Mode Based Extremum Seeking Control via Periodic Switching Function and Cyclic Search

Considering the same problem statement introduced in section 2.1, including assumptions (A1)–(A4), a new multivariable extremum seeking control approach based on sliding mode and cyclic search for static nonlinear maps is proposed. Classical and even similar methods are characterized by possible slow convergence rates and local or semi-global convergence/stability properties. On the other hand, the proposed approach via periodic switching function guarantees global and fast convergence to a neighborhood of the extremum of the objective function, due to following motivations: (1) it does not employ averaging and singular perturbation analysis tools and (2) in the control law, a sliding manifold with integral action is designed. This allows the output to track rapidly the reference signal, regardless of recurrent changes of the search direction. Stability and convergence properties are proved using Lyapunov stability analysis. Furthermore, the analysis of the residual oscillations around the extremum is carried out. Numerical simulations are performed to illustrate the theoretical results and highlight the advantages of the proposed strategy in terms of robustness, fast convergence and small residual errors. As in section 2.1, for each solution of (2.2) there exists a maximal time interval of definition given by $[0, t_M)$, where t_M may be finite or infinite.

3.1 Control Design

The proposed control approach based on sliding modes with periodic switching function and cyclic search is given by

$$u = \rho(t)\nu(t)\text{sgn}\left(\sin\left[\frac{\pi}{\varepsilon}\sigma(t)\right]\right), \tag{3.1}$$

where $\nu(t) \in \mathbb{R}^n$ is the directional cyclic search defined as in section 2.3, $\rho(t) > 0$ is a scalar modulation function, to be defined in sections 3.2, and

$$\sigma(t) = e(t) + \lambda \int_0^t \text{sgn}(e(\tau))d\tau\,, \tag{3.2}$$

with $\lambda, \varepsilon > 0$ being appropriate constants and $e(t)$, the tracking error. Note that we have just changed the variable $\sigma(t)$ to $\nu(t)$ for directional cyclic search to allow $\sigma(t)$ being the sliding surface.

Figure 3.1 illustrates the proposed control scheme based on sliding modes and periodic switching function.

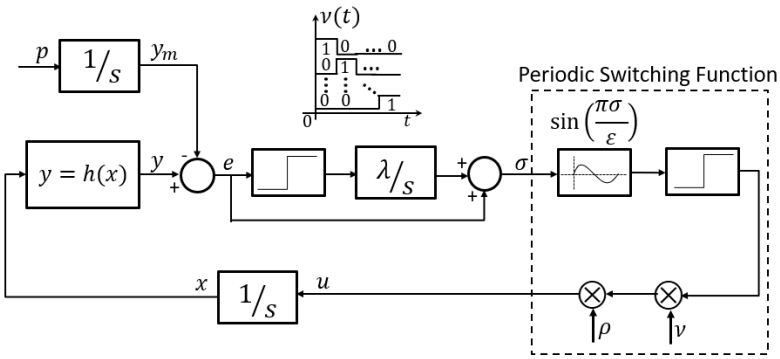

Figura 3.1: Block diagram for implementation of MESC via cyclic search and periodic switching function.

The tracking error $e(t)$ is defined as in section 2.2, repeated here for convenience,

$$e(t) = y(t) - y_m(t)\,, \tag{3.3}$$

where $y_m > 0$ is a simple ramp time-function generated by the reference model

$$\dot{y}_m = p, \quad y_m(0) = y_0\,, \tag{3.4}$$

where $p > 0$ is a design constant, y_0 is the first measurement of the output y. In order to avoid an unlimited reference trajectory $y_m(t)$ in the controller, one can saturate

it, i.e, an upper bound for the reference is considered with some value greater than y^*.

The modulation function $\rho(t)$ will be designed so that $y(t)$ can track $y_m(t)$, $\forall t$, until the output reaches the desired extremum. Thus, y is forced to reach the vicinity of the directional extrema until the global extremum $y^* = h(x^*)$ is reached and remain around it thereafter. For this purpose, a new modulation function $\rho(t)$ is proposed such that the sliding-mode $\dot{\sigma} = 0$ occurs in finite time in one of the manifolds $\sigma = k\varepsilon$, for some integer k to be defined later on.

By assuming that the following analysis takes place within a generic cycle, we neglect the cycle counter κ.

Considering the ith searching direction is active, from (3.2), one has

$$\dot{\sigma} = \dot{e} + \lambda \operatorname{sgn}(e) = 0. \tag{3.5}$$

Thus, the tracking error e is guaranteed to tend to zero, i.e., $y = h(x)$ tracks y_m (and consequently), y must approach the directional extrema y_i^* while y remains outside the vicinity of y_i^*, where the high-frequency gain is different from zero. In contrast, once y reaches the vicinity of y_i^* or y^*, the HFG will approach to zero, which leads to loss of controllability. Consequently, the tracking of y_m will cease in the ith search direction, until it is switched to another, where y_i^* is controllable, so the output tracks again the reference, and so on, until the global maximum y^* is reached as desired. The control strategy guarantees that y remains close to y^*, $\forall t$.

Remark 2 *It is important to note that in [2], the sliding manifold σ in (3.2) is designed without the integral term, i.e., $\sigma(t) = e(t)$, so there is no exact trajectory tracking, whereas in our approach it is guaranteed by adjusting the parameter λ, which leads to the convergence rate depending on the ramp parameter p and λ, while in [2] it depends on p and y_{m0}. Moreover, the integral term allows for better transients and one can saturate the reference signal without affecting the convergence to the extremum.*

To avoid repetition, please consider the design of cyclic search mechanism and assumption (A4), as in section 2.3. However, the parameter Δ and Δ_i are now related with the parameter ε, defined in equation (3.1), so that $||x - x^*|| < \varepsilon$ in $\mathcal{D}_\Delta$ and $|x_i - x_i^*(\kappa_i)| \leq \varepsilon$ in the ith directional domain $\mathcal{D}(\kappa_i)_{\Delta_i}$.

3.2 Design of the modulation function

From the objective function (2.3) and equations (3.3)-(3.4), the time-derivative of the manifold $\sigma(t)$ is given by:

$$\dot{\sigma} = \sum_{i=1}^{n} \frac{\partial h}{\partial x_i} u_i - p + \lambda \operatorname{sign}(e)\,, \tag{3.6}$$

which for the ith searching direction yields,

$$\dot{\sigma} = k_{p_i}(x)(u_i + d_\sigma)\,, \tag{3.7}$$

where

$$d_\sigma := \left(k_{p_i}(x)\right)^{-1} \left(-p + \lambda \operatorname{sgn}(e)\right)\,. \tag{3.8}$$

Now, we design the modulation function ρ in order to satisfy

$$\rho \geq |d_\sigma| + \delta, \tag{3.9}$$

with $\delta > 0$ being a constant arbitrarily small.

Suppose that we start at $t = \tau_i$, at the beginning of the ith sub-period, we have controllability of the error, with $k_{p_i} \geq L_h(\Delta_i)$, to be referred as the *condition of controllability* (see assumption (A4)). Considering d_σ as a perturbation, it can be upper bounded in absolute value by

$$\bar{d}_\sigma := L_h^{-1}\,(p + \lambda) \geq |d_\sigma|\,, \tag{3.10}$$

which allows one to define the modulation function ρ as

$$\rho = L_h^{-1}\,(p + \lambda) + \delta. \tag{3.11}$$

Note that the sliding surface dynamic analysis and modulation function design are, somehow, similar to that presented in section 2.4, i.e., equations (2.12) and (3.6), equations (2.15) and (3.10), respectively.

In order to guarantee the existence and uniqueness of the solutions of (2.2)–(2.3), the control law should be designed so that the closed-loop system satisfies the local Lipschitz condition required in Filippov's theory on each side of a sliding surface. This is indeed the case for the feedback law (3.1)–(3.2), provided $k_{p_i}(x)$ is locally Lipschitz continuous and this is guaranteed by assumption (A1).

Proposition 2 *Consider the system (2.2)–(2.3), control law (3.1)–(3.2), reference trajectory (3.4) and let $t_{\sigma_i} < \tau_i(\kappa) + \Delta\tau$ be a finite sliding mode's reaching time. For the modulation function ρ defined in (3.11), then, for the ith directional search, while $x \notin \mathcal{D}_{\Delta_i}, \mathcal{D}_{\Delta}$, one has:* ***(a)*** *the sliding-mode $\sigma = k\varepsilon$ is reached in finite time, for some integer k, regardless of the search direction,* ***(b)*** *no finite-time escape occurs in the closed loop ($t_M \to +\infty$).*

Proof. First, for any real α, one has $\lfloor\alpha\rfloor \leq \alpha < \lfloor\alpha\rfloor + 1$, where $\lfloor\alpha\rfloor$ denotes the greatest integer lower or equal to α [54].

Now, consider a non-negative Lyapunov-like function:

$$V(\sigma(t)) = \frac{(\sigma(t) - k\varepsilon)^2}{2}, \tag{3.12}$$

with $\sigma(t)$ in (3.2) and k an integer to be defined in the following. From (3.7)-(3.8) and (3.12), the time derivative of $V(t) = V(\sigma(t))$ can be written as

$$\begin{aligned}
\dot{V}(t) =& (\sigma(t) - k\varepsilon)\dot{\overbrace{(\sigma(t) - k\varepsilon)}} \\
\dot{V}(t) =& (\sigma(t) - k\varepsilon)\left[\sum_{i=1}^{n} \frac{\partial h}{\partial x_i}(u_i + d_\sigma)\right],
\end{aligned}$$

which for the ith directional search reduces to

$$\dot{V}(t) = (\sigma(t) - k\varepsilon)\left[k_{p_i}\left(\rho\text{sgn}\left(\sin\left[\frac{\pi}{\varepsilon}\sigma(t)\right]\right) + d_\sigma\right)\right]. \tag{3.13}$$

From the definition above, the inequality

$$k\pi \leq \frac{\pi}{\varepsilon}\sigma < (k+1)\pi, \quad k := \lfloor\frac{\sigma(t)}{\varepsilon}\rfloor,$$

holds $\forall t \in [0, t_M)$. Therefore, in the neighborhood of k, one has $\sin\left[\frac{\pi}{\varepsilon}\sigma(t)\right] \geq 0$ for an even k and $\sin\left[\frac{\pi}{\varepsilon}\sigma(t)\right] < 0$ for an odd k. Note that the function (3.12) is more restrictive than that considered in [14, Appendix B], a triangular-wave function which is valid for all k, however, it is enough for the desired demonstration. Thus, the control signal u in (3.1) can be rewritten as

$$u_i = \rho\text{sgn}\left(\sin\left[\frac{\pi}{\varepsilon}\sigma(t)\right]\right) = \rho(-1)^k. \tag{3.14}$$

Thus, (3.13) can be rewritten as

$$\dot{V}(t) = (\sigma(t) - k\varepsilon)\left[k_{p_i}\left(\rho(-1)^k + d_\sigma\right)\right]. \tag{3.15}$$

It is known that $k_{p_i} = |k_{p_i}| \operatorname{sgn}(k_{p_i})$, then

$$\dot{V}(t) = |k_{p_i}| \left(\rho(-1)^k \operatorname{sgn}(k_{p_i})(\sigma(t) - k\varepsilon)\right) + |k_{p_i}| \left(d_\sigma \operatorname{sgn}(k_{p_i})(\sigma(t) - k\varepsilon)\right). \tag{3.16}$$

On the other hand, it was shown in [14, Appendix B], for scalar ESC, that $\operatorname{sign}(k_p) < 0$ corresponds to an even k and $\operatorname{sign}(k_p) > 0$ occurs for an odd k, which is also valid for $\operatorname{sign}(k_{p_i})$, i.e., for the ith search direction, so one has in (3.16) $(-1)^k \operatorname{sgn}(k_{p_i}) = -1$, independently of $\operatorname{sign}(k_{p_i})$. Thus,

$$\begin{aligned}
\dot{V}(t) &= |k_{p_i}| \left[-\rho(\sigma(t) - k\varepsilon) + d_\sigma \operatorname{sgn}(k_{p_i})(\sigma(t) - k\varepsilon)\right] \\
&\leq |k_{p_i}| \left[-\rho|(\sigma(t) - k\varepsilon)| + |d_\sigma||(\sigma(t) - k\varepsilon)|\right] \\
&\leq |k_{p_i}| \left(-\rho + |d_\sigma|\right)|(\sigma(t) - k\varepsilon)|
\end{aligned}$$

Since the modulation function ρ satisfies (3.9) and $|\underline{k}_{p_i}| > L_h$ (see (2.11)), the following inequality holds $\dot{V}(t) \leq -L_h|(\sigma(t) - k\varepsilon)|\delta < 0$, and the condition

$$(\sigma(t) - k\varepsilon)\dot{\overbrace{(\sigma(t) - k\varepsilon)}} < 0,$$

is verified such that an ideal sliding-mode occurs on the manifold $\sigma(t) - k\varepsilon = 0$, or equivalently, on the manifold $\sigma(t) = k\varepsilon$ in finite time, while $x \notin \mathcal{D}_{\Delta_i}$. Hence, there exists a finite time $t_{\sigma_i} < \tau_i(\kappa) + \Delta\tau$ (see (2.10)) such that $\sigma(t) = k\varepsilon$, independently of $\operatorname{sign}(k_{p_i})$.

The sliding mode reaching time t_{σ_i} can be easily calculated by supposing that at $t = t_{\sigma_1}$, the surface $\sigma(t_{\sigma_1}) = k\varepsilon$ is reached. Then, for $\sigma(0)$ one has

$$|\sigma(0) - \sigma(t_{\sigma_1})| = |\sigma(0) - k\varepsilon| \leq \varepsilon\,,$$

Thus, the reaching time for the first search direction can be defined as follows [2]:

$$|t_{\sigma_1}| = \frac{|\sigma(0) - \sigma(t_{\sigma_1})|}{|\dot{\sigma}(t)|} \tag{3.17}$$

$$= \frac{|\sigma(0) - k\varepsilon|}{|\frac{dh}{dx_1}\rho \operatorname{sgn}(\sin\left(\frac{\pi\sigma(t)}{\varepsilon}\right)) + p|} \tag{3.18}$$

$$\leq \frac{\varepsilon}{L_h\rho + p}\,. \tag{3.19}$$

This means that for the first search direction, i.e. $t \in [\tau_1, \tau_2)$, the sliding-mode is reached with $t_{\sigma_1} < \tau_2$. Since these steps are valid for all directions, i.e., $i = 1, 2, \cdots, n$, then the output does not escape in finite-time, $t < t_M$, provided in (2.10), the searching time $\Delta\tau_i > \frac{\varepsilon}{L_h\rho+p}$. ■

3.3 Main Result - Global Convergence

In this section, the main result of the proposed output feedback multivariable controller based on a periodic switching function and cyclic search is presented. It is shown that the proposed approach drives x to $\mathcal{D}_\Delta$ of the unknown maximizer x^* defined in assumption (A2) and guarantees that the oscillations around y^* can be made of order $\mathcal{O}(\varepsilon)$.

Theorem 2 *Consider the system (2.2)–(2.3), control law (3.1)–(3.2), reference model (3.4) and modulation function (3.9). Assume that assumptions (A1)–(A4) hold, then:* ***(i)*** *the regions $\mathcal{D}_{\Delta_i}$ and $\mathcal{D}_\Delta$ in (A4) are globally attractive, being reached in finite time and* ***(ii)*** *for L_h sufficiently small, the oscillations around y^* can be made of order $\mathcal{O}(\varepsilon)$.*

Proof. In what follows, we present the proofs of properties **(i)** and **(ii)** of Theorem 2. This proof correspond to the generalization of our previous results on scalar ESC [14] to the multivariable scenario.

(i) The regions $\mathcal{D}_{\Delta_i}$ and $\mathcal{D}_\Delta$ in (A4) are globally attractive, being reached in finite time.

The proof is made by contradiction. Assume that $x(t)$ stay outside the regions $\mathcal{D}_{\Delta_i}$ and $\mathcal{D}_\Delta$ $\forall t$, i.e., $x \notin \mathcal{D}_{\Delta_i}, \mathcal{D}_\Delta$. According to Proposition 2, for each search direction, there exists a finite-time $t_{\sigma_i} < \tau_i(\kappa) + \Delta\tau$, such that $\sigma = k\varepsilon$, $\forall t > t_{\sigma_i}$, $\forall\kappa$th cycle. Thus, $\dot{\sigma} = 0$ and from (3.2), one has that $\dot{e} = -\lambda\,\mathrm{sgn}(e)$, $\forall t > t_{\sigma_i}$. This means that, unlike [2], the tracking error $e = y - y_m \to 0$, but since y_m strictly increases with time and $y = h(x)$ has a directional maximum value y_i^*, for t large enough but less than $\tau_i(\kappa) + \Delta\tau$, $y_m > y_i^* > y$ and $\mathrm{sign}(e) = -1$, assuring that y increases with constant rate $\dot{y} = p + \lambda$, such that y must approach y_i^*. So, x is driven inside $\mathcal{D}_{\Delta_i}$, which is a contradiction. Thus, $\mathcal{D}_{\Delta_i}$ is attained in some finite time. Consequently, $x(t)$ remains or oscillates around $\mathcal{D}_{\Delta_i}$, and similarly y with respect to some small vicinity of y_i^*, $\forall t$ large enough. These oscillations come from the loss of controllability of k_{p_i} whenever the relation $\underline{k}_{p_i} \leq |k_{p_i}|$ is violated, or are due to the recurrent changes in the HFG signal at the extremum point (y_i^*, x_i^*), where $k_{p_i} = 0$. During these oscillations, σ can go from one sliding manifold $\sigma = k\varepsilon$ (k even when $\mathrm{sgn}(k_{p_i}) < 0$) to another ($k$ odd when $\mathrm{sgn}(k_{p_i}) > 0$). As the sliding-modes occur in all searching directions, by continuity, the region $\mathcal{D}_\Delta$ is attained in finite time $t < t_M$, i.e, $x(t)$ remains or oscillates around x^*. In what follows, we show that these oscillations can be made of order $\mathcal{O}(\varepsilon)$, with ε defined in (3.1).

(ii) for L_h sufficiently small, the oscillations around y^* can be made of order $\mathcal{O}(\varepsilon)$.

For ith search direction and κth cycle, $y(t)$ follows a ramp with increasing rate

p (from reference trajectory) until it reaches the directional extremum, i.e., in the region $\mathcal{D}_{\Delta_i}$.

Assume that x reaches the frontier of $\mathcal{D}_{\Delta_i}$ (from inside) at some time $t_1 > t_{y_i^*}$, where $t_{y_i^*}$ is the time which any directional maximum y_i^* is reached, and assume also that $\sigma(t)$ is not in sliding mode at $t = t_1$. As we referred in the property **(i)**, for $t > t_{y_i^*}$ one has $\text{sgn}(e) = -1$, since, y_m strictly increases with time and y has a directional maximum y_i^*. Therefore, one can conclude from (3.2) that

$$\sigma(t) = y - y_m - \lambda t + C, \quad \forall t > t_{y_i^*} \tag{3.20}$$

where $C = \lambda[t_{y_i^*} + \int_0^{t_{y_i^*}} \text{sign}(e(t = \tau))d\tau]$ is a constant. Moreover, from (3.20) one can write

$$\tilde{\sigma}(t) = \tilde{y}(t) - (\delta_m + \lambda)(t - t_1), \quad t > t_1, \tag{3.21}$$

where $\tilde{\sigma}(t) := \sigma(t) - \sigma(t_1)$, $\tilde{y}(t) := y(t) - y(t_1)$, $\delta_m = 0$ when y_m is saturated and $\delta_m = p$, otherwise. In addition, from (3.21) one can also write

$$|\tilde{y}(t)| \leq |\tilde{\sigma}(t)| + [\delta_m + \lambda](t - t_1), \quad t > t_1. \tag{3.22}$$

Let $t_2 \geq t_1 > t_{y_i^*}$ and $t_3 \geq t_1 > t_{y_i^*}$, where t_2 is the first time when $\sigma(t)$ reaches the next sliding manifold $\sigma(t) = \sigma(t_2)$ (independently if $x(t)$ is inside or outside $\mathcal{D}_{\Delta_i}$) and t_3 is the first time when $x(t)$ reaches the frontier of $\mathcal{D}_{\Delta_i}$ again (from outside). Notice that $x(t) \notin \mathcal{D}_{\Delta_i}, \mathcal{D}_{\Delta}$, for $t \in [t_1, t_3)$.

Now, consider two cases: (a) x reaches the frontier of $\mathcal{D}_{\Delta_i}$ with σ in sliding motion ($t_3 > t_2$) and (b) x reaches the frontier of $\mathcal{D}_{\Delta_i}$ with σ not in sliding motion $t_3 \leq t_2$.

In both cases there is a time interval $[t_1, t_2)$ where $\sigma(t)$ is not in sliding motion before x reaches the frontier of $\mathcal{D}_{\Delta_i}$: for case (a) one has $[t_1, t_2) = [t_1, t_3)$, i.e. $t_2 = t_3$ and for case (b) one has $[t_1, t_2)$ one has $[t_1, t_2) \subset [t_1, t_3)$, i.e. $t_2 < t_3$.

Thus, $\sigma(t)$ is not in sliding motion $\forall t \in [t_1, t_2)$. Consequently, one has $(k-1)\varepsilon < \sigma(t) < k\varepsilon$, for some integer k. Otherwise, sliding mode occurs at $\sigma(t) = (k-1)\varepsilon$ or $\sigma(t) = k\varepsilon$, according to Proposition 2. Therefore, $\tilde{\sigma}(t) = \sigma(t) - \sigma(t_1)$ is of order $\mathcal{O}(\varepsilon)$. Moreover, $t_2 - t_1$ is of order $\mathcal{O}(\varepsilon)$, also from Proposition 2. Thus, by continuity, $\tilde{y}$ is of order $\mathcal{O}(\varepsilon)$, $\forall t \in [t_1, t_2)$, and $\tilde{y}(t_2) \approx \tilde{y}(t_1)$.

For case (b), suppose $t \in [t_1, t_3]$. During this time interval σ is not in sliding motion. Thus, one can also conclude that $\tilde{y}(t)$ is of order $\mathcal{O}(\varepsilon)$, $\forall \in [t_1, t_3]$, following directly the steps of the first part of the proof of case (a). Note that, the time interval $[t_2, t_3)$, when σ is in sliding mode, depends on the design of parameters p and λ, while the time interval $[t_1, t_2)$, when σ is not in sliding mode, is of order

$\mathcal{O}(\varepsilon)$. By the continuity of the uncertain output function $h(x)$, the boundedness of y stated in the Assumption (A3) implies that x is uniformly norm bounded ($\mathcal{UB}$), and also one can easily conclude that all closed-loop system signals are $\mathcal{UB}$, except for σ, since from (3.20), $|\sigma| \to +\infty$ as $t \to \infty$. However, this phenomenon is not harmful, since σ is only a modified timescale for the argument of the sine function in (3.1). ■

3.4 Illustrative Example

In order to evaluate the performance of the proposed approach, the simulation study is performed for the same numerical example in the section 2.8, repeated here for convenience.

Consider a two-input nonlinear plant where the objective function is unknown in cascade with a simple integrator described by

$$\dot{x} = u\,, \tag{3.23}$$

$$y = -(x_1^2 + (x_2 - x_1^2)^2)\,. \tag{3.24}$$

with optimum parameters $x^* = (0, 0)$ and $y^* = 0$. The control law (3.1)–(3.2) can be applied with the modulation function ρ satisfying (3.9). The simulation parameters were chosen as $p = 0.5$, $\varepsilon = 0.02$, $T_s = 0.5s$, $L_h = 0.6$, $\delta = 0.1$, $\lambda = 5$ and $y_{m0} = -2$. Applying these parameters in (3.9) yields the modulation function $\rho = 9.3$.

Figure 3.2 illustrates the proposed extremum seeking approach tracking and remaining at the vicinity of extremum point $x^* = (0, 0)$ and $y^* = 0$, when the initial condition is chosen as $x(0) = (-1.5, 1.5)$. In the zoomed figure, one can note that the oscillations around x^* are indeed of order $\mathcal{O}(\varepsilon)$.

Figure 3.3 illustrates the time evolution of the plant output, following the reference trajectory in sliding-mode, except when the output reaches the ith directional maximum or the global one at $y^* = 0$. The dashed-line in black is the result by implementing the approach proposed in [2]. Note that, after saturating the ramp, it stops searching the extremum because the argument of the periodic switching function becomes constant. Thus, our approach seems to be faster and more robust to the variations on the reference trajectories. The control signals u_1 e u_2 and the periodic searching direction ν_1 and ν_2 with period $T_s = 0.5s$ are shown in Figure 3.4.

From Figure 3.3, in a scenario where the initial condition of the reference is less (in absolute value) than the first measurement of the output, the convergence of the proposed approach may be slower than in [2]. This dependence on the initial condition can be solved in both approaches by setting the reference at $y_{m0} = y(0)$. However, even in this scenario, the speed of convergence in [2] will be slower because,

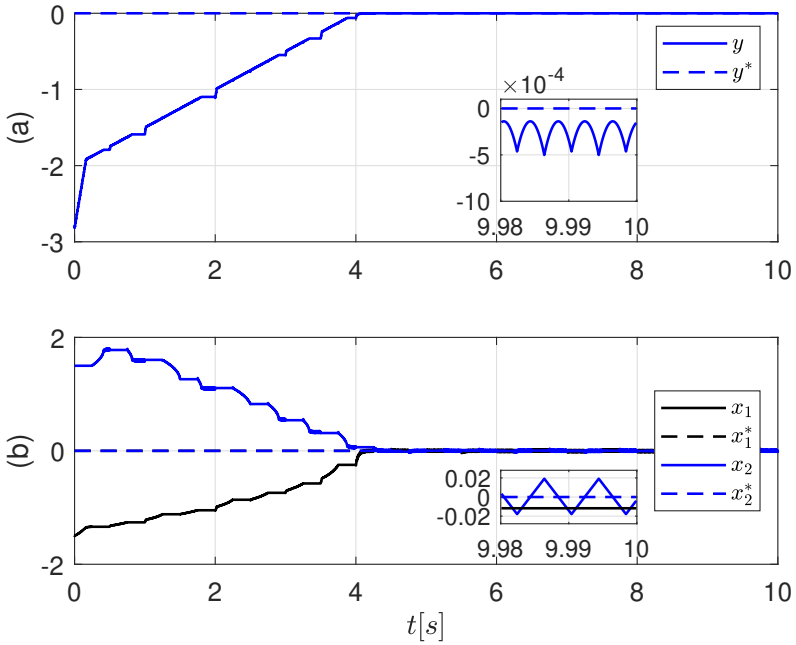

Figura 3.2: In (a) the output of the plant converges to a small neighborhood of $y^* = 0$ and (b) the input vector x converges to a small neighborhood of $x^* = (0, 0)$, when the initial condition is chosen as $x(0) = (-1.5, 1.5)$.

after each change of the search direction, a new sliding mode occurs, in which $e(t) =$ *constant* in [2] while $e(t) \to 0$ in our approach, i.e., we guarantee the tracking of the reference regardless of the search direction. In other words, here, the convergence depends on the parameters p and λ, whereas in [2] just on p.

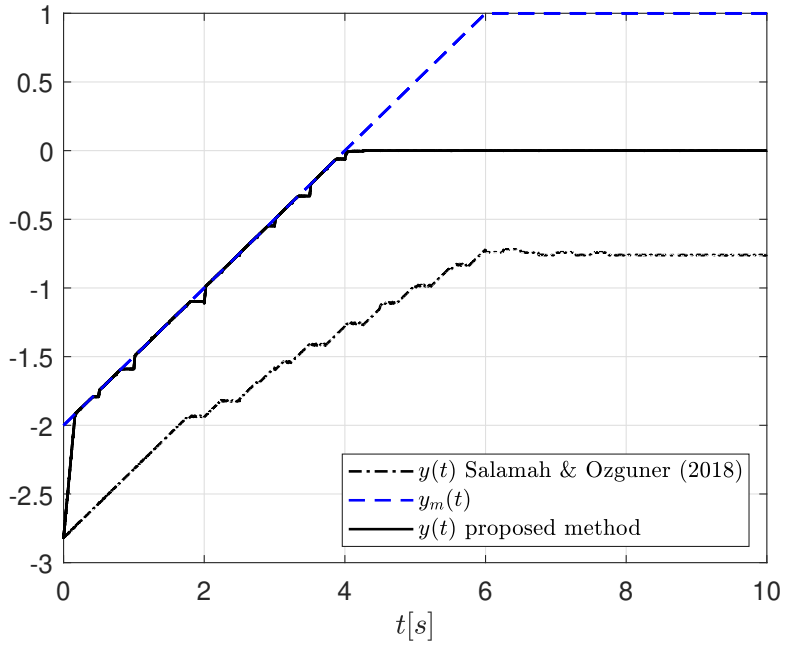

Figura 3.3: The plant output $y(t)$ tracks the reference trajectory $y_m(t)$ in sliding-mode crossing several directional maximum until reaching $y^* = 0$, while the strategy proposed in [2] does not do it due to the saturation.

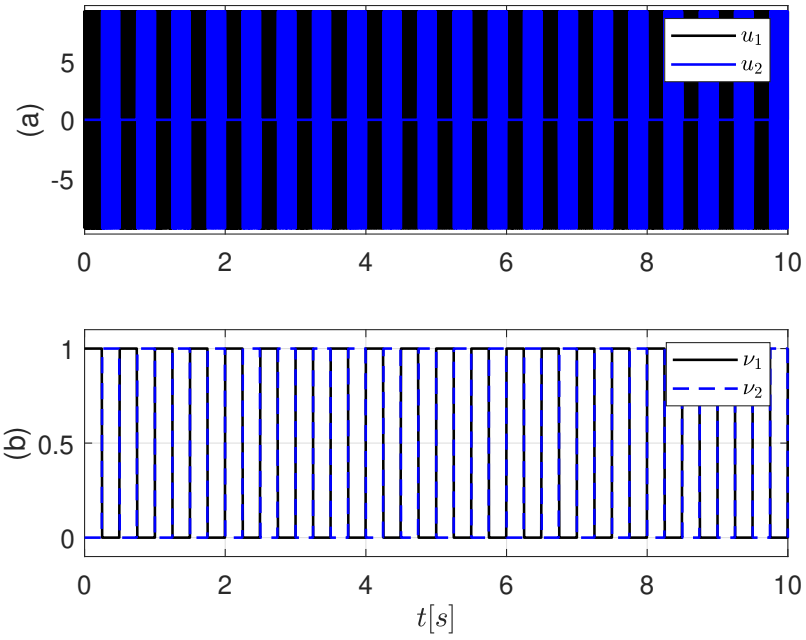

Figura 3.4: (a) control signals u_1 e u_2 and (b) the cyclic search direction with period $T_s = 0.5s$.

3.5 Conclusion

A novel multivariable sliding-mode extremum seeking control via cyclic search and periodic switching function was introduced for a class of uncertain nonlinear multivariable static plants. The resulting approach guarantees global finite-time convergence of the system output to a small neighborhood of the extremum point. Convergence and stability properties were provided via Lyapunov stability analysis. The main contribution was to relax some stringent assumptions considered in the literature and modify the periodic switching function in order to guarantee faster convergence properties. Moreover, a complete analysis of the oscillations around the extremum was considered. Simulation results were carried out to illustrate the remarkable controller performance.

Capítulo 4

Multivariable Extremum Seeking for Dynamic Maps with Arbitrary Relative Degree

In [15, 71], it was introduced the extension of our results on ESC with dynamic systems from relative degree one [13] to arbitrary relative degree. However, the authors considered only SISO linear systems. Hereafter, we introduce the extension to multivariable extremum seeking control with arbitrary relative degree plants, by considering linear dynamic systems.

It is known that one solution for relative degree mitigation in extremum seeking problems is achieved by means of a time-scaling technique and singular perturbation method. Thus, we show that in the new time-scale, an attractive manifold is revealed, which essentially reduces the considered system to a single integrator perturbed by a fast sensor dynamics, which in turn ultimately converges to a small residual set. We then exploit this particular structure to redesign, with reduced control authority, our control law (2.7) to show its robustness with respect to the arbitrary relative degree dynamics at the expense of some time dilation, which slows down the system response.

Although in this chapter we will address the generalization to dynamical maps with arbitrary relative degree using the method based on monitoring function (chapter 2), the same approach to be presented below can also be applied to the method based on periodic switching function (chapter 3), since the theoretical results of both methods are similar.

In this sense, we intend to show that the MESC proposed in chapter 2, in the light of our scalar approach [15], can also be extended to multi-input systems with

uncertain and arbitrary relative degree (n^*) in the form:

$$\dot{v} = u\,, \tag{4.1}$$
$$\dot{x} = Ax + Bv \tag{4.2}$$
$$z = Cx\,, \tag{4.3}$$

in cascade with a static subsystem

$$y = h(z)\,, \tag{4.4}$$

where $u \in \mathbb{R}^m$ is the control input, $x \in \mathbb{R}^n$ is the state vector, $z \in \mathbb{R}^n$ is an unmeasured output of the linear subsystem (4.1)–(4.3) and $y \in \mathbb{R}$ is a measured output of the static subsystem (4.4), respectively.

4.1 Basic Assumptions

The matrices $A \in \mathbb{R}^{n\times n}$, $B \in \mathbb{R}^{n\times m}$, $C \in \mathbb{R}^{n\times n}$ and the order n of the subsystem (4.2) may also be uncertain. The uncertain nonlinear function $h : \mathbb{R}^n \to \mathbb{R}$ to be maximized must still satisfy assumptions (A1)-(A4).

The following assumptions are further assumed:

(A5) (*On the uncertainties*): All the uncertain plant parameters belong to a compact set Ω.

(A6) (*On the linear subsystem*): The matrix A in (4.2) must be Hurwitz.

(A7) (*On the DC gain of the linear subsystem*): The DC gain of the linear subsystem (4.2)–(4.3) verifies $\|CA^{-1}B\| \geq \underline{k}_{DC} > 0$ for some known constant $\underline{k}_{DC}$.

These assumptions are necessary to obtain the uncertainty bounds for the control design.

4.2 Singular Perturbation Analysis

In order to present such generalization, consider the system (2.2)–(2.3), written in the following form

$$\dot{v} = u\,, \tag{4.5}$$
$$y = h(v)\,, \tag{4.6}$$

can be directly controlled by the method of monitoring function described in section 2.5.

By using the singular perturbation approach [72], it can be shown that extremum seeking control based on monitoring function [13] is robust to fast unmodeled dynamics such that the perturbed system (4.5)–(4.6) is rewritten in the following *block sensor form* [72, p. 50]

$$\begin{aligned} \dot{v} &= u\,, && (4.7)\\ \eta\dot{x} &= Ax + Bv\,, && (4.8)\\ y &= h(Cx)\,, && (4.9) \end{aligned}$$

and ultimately satisfies the inequality

$$|y - y^*| \leq \mathcal{O}(\sqrt{\eta} + \mu^2)\,, \tag{4.10}$$

where $\eta > 0$ and $\mu > 0$ are sufficiently small constants. The complete demonstration of (4.10) follows the similar steps presented in [73].

In the singular case $\eta = 0$, the differential equation (4.8) is replaced by the algebraic equation $x = -A^{-1}Bu$ and, from (4.7) and (4.9), the first time derivative of the output signal y is given by

$$\dot{y} = k_p(z)u\,, \tag{4.11}$$

where the HFG is now rewritten as

$$k_p(z) = -h'(z)CA^{-1}B\,. \tag{4.12}$$

From (4.12) and assumption (A4), $k_p(z)$ satisfies

$$0 < \underline{k}_p \leq \|k_p(z)\|\,,\ |k_{p_i}(z)|\,; \tag{4.13}$$

where $\underline{k}_p \leq L_h\|CA^{-1}B\|$ is a known constant lower bound for the HFG, considering all the admissible uncertainties in $h(\cdot)$, A, B, and C.

4.3 Time-Scaling for Control Redesign

By applying an appropriate linear time-scaling [71]

$$\frac{dt}{d\tau} = \eta\,, \tag{4.14}$$

the system (4.7)–(4.9) can be rewritten as

$$v' = \eta u \tag{4.15}$$
$$x' = Ax + Bv\,, \tag{4.16}$$
$$z = Cx\,, \tag{4.17}$$
$$y = h(z)\,, \tag{4.18}$$

where $v' := \dfrac{dv}{d\tau}$ and $x' := \dfrac{dx}{d\tau}$. It means that $\exists \eta^* > 0$ such that the input signal u can be scaled (4.15) to control the original system (4.2)–(4.4) in a different dilated time-scale governed by $t = \eta\tau$, $\forall \eta \in (0, \eta^*]$.

The physical meaning is that since the monitoring function based ESC originally proposed for systems with relative degree one is robust to fast unmodeled stable dynamics ($\eta \to +0$), then it is also adequate to control arbitrary relative degree dynamics, if properly scaled. As expected, the price to be paid is that the closed-loop system response slows down as $\eta \to +0$.

When $\eta \neq 0$ in (4.8), the time-scaling (4.14), allow us to consider the original plant (4.2)–(4.4) in a different time-scale being controlled by the controller (2.7) properly scaled by ηu, see (4.15).

In order to incorporate it, the modulation function must be redesigned to satisfy

$$\rho = \eta[\bar{d}_e + \gamma], \tag{4.19}$$

instead of (2.17).

From the singular perturbation analysis sketched in section 4.2, if (2.7) was used again, an upper bound for the tracking error $e(t)$ could be directly obtained, for η sufficiently small, by adding the steady-state and transient terms in (4.10) and (2.19), respectively:

$$|e(t)| \leq \zeta(t)\,, \quad \zeta(t) := |e(\tau_1)|e^{-\lambda(t-\tau_1)} + \pi_e + \mathcal{O}(\sqrt{\eta} + \mu^2), \tag{4.20}$$

where π_e is an exponentially fast decaying term which encompass the effect of the stable unmodeled dynamics (4.8).

If we knew the control direction ($\mathrm{sgn}(k_{p_i})$) one could implement the control law (2.7). Thus, based on the monitoring function designed in section 2.5, equation (2.20) one can rewrite the control law (2.7) for the ith search direction on the system (2.2)–(2.3) yielding the following sliding-mode control law (2.16), repeated here for convenience

$$u_i = -\rho U(t)\,\mathrm{sgn}(e)\,, \quad u_j = 0\,, \quad \forall j \neq i\,, \quad \text{and} \quad i\,, j \in \{1, \ldots, n\}\,, \tag{4.21}$$

with new modulation gain ρ defined in (4.19), $U(t) = +1$ or -1, according to the estimated sign of k_{p_i}. If correctly estimated, $U = \text{sign}(k_{p_i})$, otherwise $U = -\text{sign}(k_{p_i})$. Notice that, the term π_e in (4.20) can be neglected in the monitoring function design since it only represents a stable and fast mode for which the controller has already been proved to be robust in section 4.2. According to the definition of monitoring function in (2.20) subject to (4.20), the ultimate residual set of oscillations will be of order $\mathcal{O}(\sqrt{\eta} + \mu^2)$.

The next proposition summarizes the new results, which are very similar to Proposition 1.

Proposition 3 *Consider the system (4.1)–(4.4), reference model (2.9), search direction (2.10), control law (2.16), monitoring function (2.20) and modulation function (4.19). Consider any arbitrary initial control direction outside of regions $\mathcal{D}_\Delta$ and $\mathcal{D}_{\Delta_i}$. Then, with the ith directional search being active, one can choose $\gamma > 0$ in (2.17) sufficiently large such that* ***(a)*** *the correct control direction is reached before the time instant $\tau_i + \epsilon$, where $\tau_i > 0$ is the beginning of the ith search direction, $\epsilon > 0$ is arbitrarily small and less than the sub-interval T_s/n and* ***(b)*** *no finite-time escape occurs in the closed-loop system.*

Proof. By considering the singular perturbation argument and the time-scaling (4.14), which show that the systems (4.7)–(4.9) and (4.15)–(4.18) are equivalent for η sufficiently small, then, the demonstration for the original plant (4.1)–(4.4) follows the same steps presented in the proof of Proposition 1 for the relative degree one case. ■

Remark 3 *Since the control design is developed in the light of the slow time-scale ηt, it is natural that the parameters p of the reference model (2.9) as well as λ in the monitoring function (2.20)–(2.22) must be rescaled appropriately as ηp and $\eta\lambda$.*

4.4 Global Convergence Result

Theorem 3 states that the proposed multivariable output-feedback controller based on monitoring function drives z to the Δ-vicinity defined in **(A4)** of the unknown maximizer z^*. It does not imply that $z(t)$ remains in $\mathcal{D}_\Delta$, $\forall t$. However, the amplitude of signal oscillations around y^* can be kept of order $\mathcal{O}(\sqrt{\eta} + \mu^2)$.

Theorem 3 *Consider the system (4.1)–(4.4), control law (2.7), reference model (2.9), search direction (2.10), modulation function (4.19) and monitoring function (2.20)–(2.22). Assume that assumptions (A1)-(A7) hold and T_s is sufficiently large. Then the region $\mathcal{D}_\Delta$ in (A4)* ***(i)*** *is globally attractive, being reached in finite time and*

(ii) *once it is reached, the oscillations around* y^* *can be made of order* $\mathcal{O}(\sqrt{\eta}+\mu^2)$ *after some finite time by choosing* Δ *sufficiently small.*

Proof. As in the proof of Proposition 3, the demonstration is based on singular perturbation/time-scaling arguments and follows the steps presented in the proof of Theorem 1 [61], for η sufficiently small. ■

4.5 Numerical Simulation Example

As an example, consider a plant whose objective function is unknown, in cascade with a linear dynamic system described by

$$\dot{v} = u\,, \tag{4.22}$$

$$\dot{x} = \begin{bmatrix} 0 & 1 \\ -4 & -2 \end{bmatrix} x + \begin{bmatrix} 1 & 0 \\ 0 & 1 \end{bmatrix} v\,, \tag{4.23}$$

$$z = \begin{bmatrix} 1 & 0 \\ 0 & 1 \end{bmatrix} x\,, \tag{4.24}$$

and an output function

$$y = h(z) = 5 - (z_1^2 + z_2^2 - 2\epsilon z_1 z_2) \tag{4.25}$$

The static map (4.25) consists of the particular representation of functions of type

$$y = h(z) = y^* + \frac{1}{2}(z - z^*)^T H (z - z^*) \tag{4.26}$$

where

$$H = \begin{bmatrix} 2 & 2\epsilon \\ 2\epsilon & 2 \end{bmatrix} < 0$$

is the Hessian matrix negative definite. It is easy to notice that the optimal parameters of the objective function (4.25) are $z^* = (0, 0)$ and $y^* = 5$, for $0 < \epsilon < 1$, condition which $h(z)$ has a maximum point.

A second simulation scenario considers the following system for the same objec-

tive function (4.25):

$$\dot{v} = u\,, \tag{4.27}$$

$$\dot{x} = \begin{bmatrix} 0 & 1 \\ -40 & -20 \end{bmatrix} x + \begin{bmatrix} 10 & 0 \\ 0 & 10 \end{bmatrix} v\,, \tag{4.28}$$

$$z = \begin{bmatrix} 1 & 0 \\ 0 & 1 \end{bmatrix} x\,. \tag{4.29}$$

The simulations were performed considering the following control system parameters: $p = 5$, $k_{pmin} = 5$, $\lambda = 20$, $\gamma = 0.1$, which result in $\rho = 5$. Other parameters: $\epsilon = 0.1$, $\mu = 0.1$, $T_s = 1s$.

Figure 4.1 shows the objective function and the trajectories converging to the extremum $y^* = 5$, from three initial conditions, $z_0 = (-2, 2)$ (black), $z_0 = (2, -2)$ (blue) e $z_0 = (-1.5, -1.5)$ (green). The input variable z and output y regarding first scenario, i.e, system (4.23)-(4.24), converging to its optimum values are illustrated in Figure 4.2.

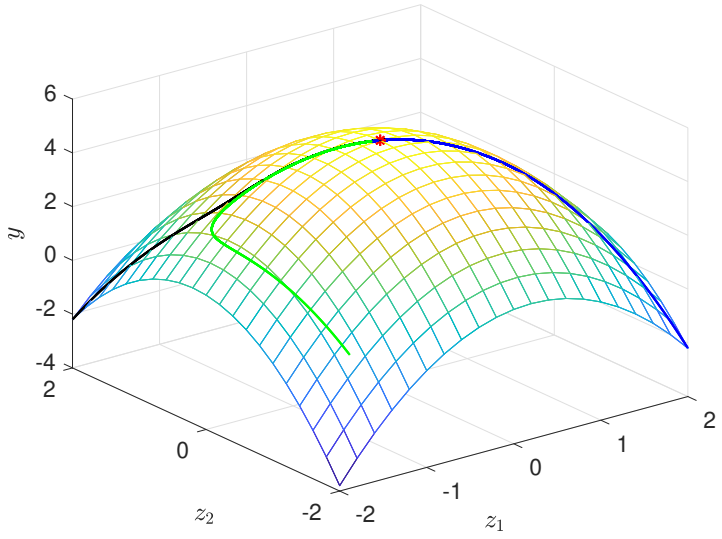

Figura 4.1: The objective function $y = h(z)$ and the tracking of the optimum point from three initial conditions.

The control signals u_1 and u_2 and the cyclic search functions σ_1 and σ_2 are illustrated in Figure 4.3, also in time-scale $t = \tau$. Note that the searching period is 1s and, therefore, 0.5s for each searching direction.

In the second scenario, is considered a new time-scale $t = \eta\tau$, with $\eta = 0.01$. As mentioned in the Remark 3, the parameters p, λ, ρ and the searching period T_s must be properly scaled, i.e., multiplied by η. Figure 4.4 shows the input and

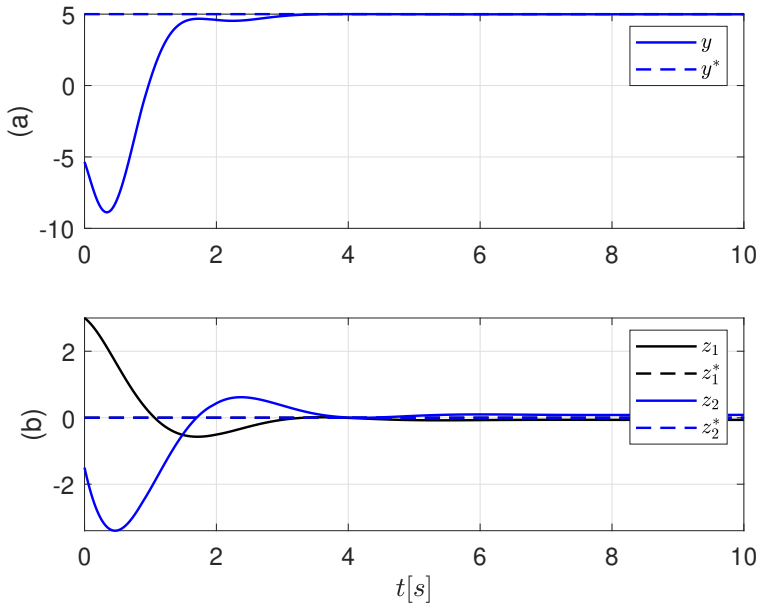

Figura 4.2: Convergence of the variables z and y to expected optimum points, $z^* = (0\,, 0)$ and $y^* = 5$, respectively, from the initial condition $z_0 = (3\,, -1.5)$, in the time-scale $t = \tau$.

output signals z and y converging to their optimal points. Note that after an initial transient, close to 50s, y tracks the reference y_m in sliding mode until z reaches the maximizer $z^* = 0$ and y reaches $y^* = 5$.

Figure 4.5 shows the monitoring function upper bounding the norm of the tracking error. After 350s, note that the reference was saturated at 10, so that the tracking error is equal to 5. In the zoomed part, it is possible to see the jumps $\mu = 0.1$, at each change in the control direction.

A limitation of using time-scaling method for compensation of relative degree, in addition to time dilation, is the fact that this method works for $\eta \to 0$, i.e, for fast unmodeled dynamics, as discussed in the introduction of chapter 4 and now is illustrated in Figure 4.6, for $\eta = 0.1$. The input z and, consequently, the output y try to find their optimal points, but the control is lost.

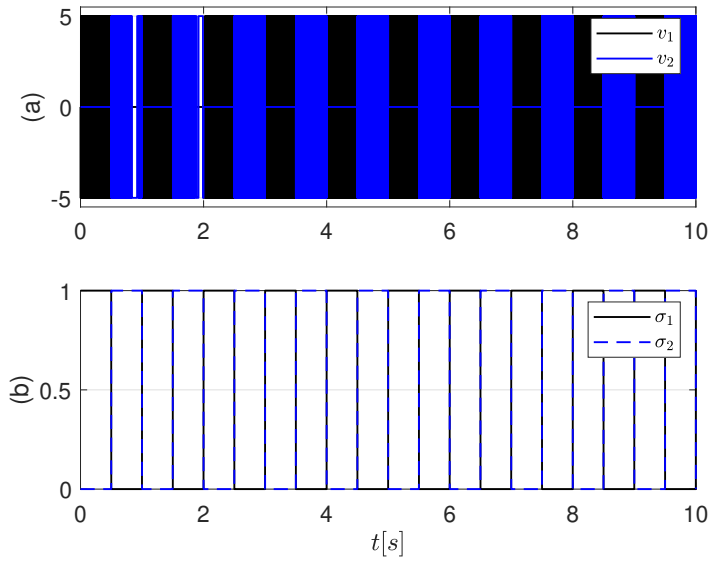

Figura 4.3: Control signals u_1 and u_2 and the cyclic searching functions σ_1 and σ_2, with period $T_s = 1$s.

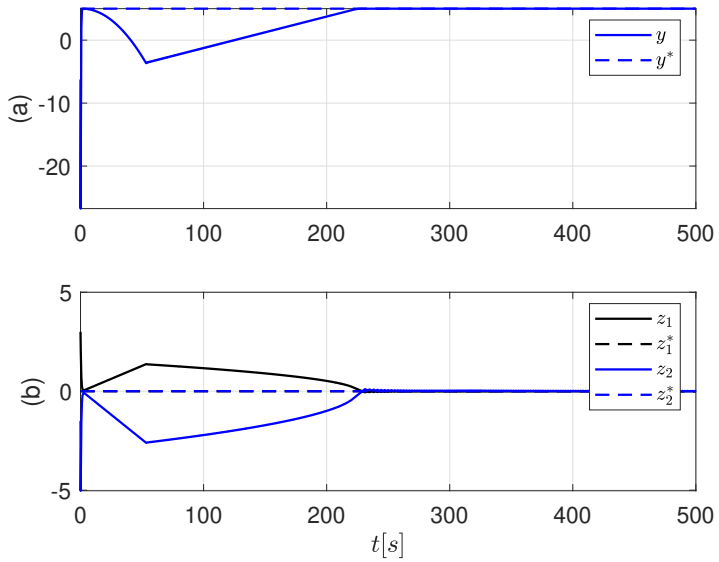

Figura 4.4: The convergence of the signals z to y their optimum points, $z^* = (0, 0)$ and $y^* = 5$, respectively, from the initial condition, $z_0 = (3\,, -1.5)$ obeying the time-scale $t = \eta\tau$.

4.6 Conclusion

In this chapter, a multivariable sliding mode based extremum seeking for dynamic mappings, with arbitrary relative degree, using monitoring function, time scaling and cyclic search was proposed. This strategy guarantees global stability and convergence for a small neighborhood of the optimal extremum of the objec-

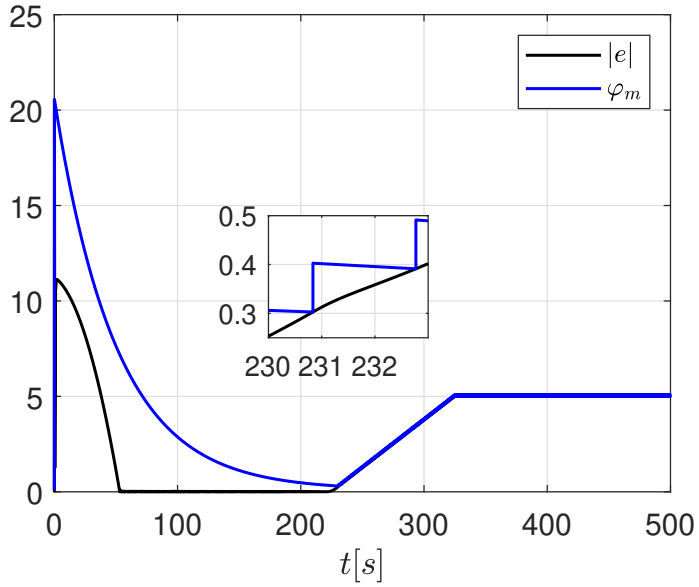

Figura 4.5: The monitoring function, upper bounding and monitoring the error norm $|e(t)|$ continuously.

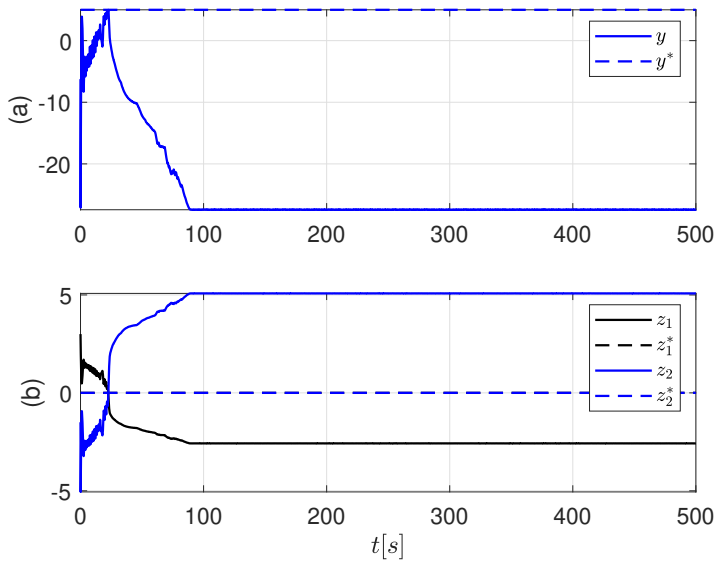

Figura 4.6: The convergence of the signals z and y to their optimum points fail as η increases ($\eta = 0.1$).

tive function. Simulations show the applicability of time-scaling in optimization problems, which brings also the disadvantage of response time delay. One strategy for nonlinear systems under the addition of slow unmodeled dynamics in view for relative degree compensation without compromising response time delay is the application of differentiators based on higher order sliding modes (HOSM) [74].

Capítulo 5

Conclusion

In this thesis, two novel methods of multivariable extremum seeking control were considered, namely extremum seeking control based on the monitoring function with cyclic search in chapter 2 and extremum seeking control based on the periodic switching function with cyclic search in chapter 3. They are extensions of our previous results [13, 43] for MISO uncertain nonlinear static plants, based purely on output feedback and sliding mode control. These approaches resulted in the following contributions:

1. The monitoring function-based method when applied to multivariable extremum seeking control leads to global convergence, despite the unknown control direction. It is shown that the oscillations around the optimum points can be made of order $\mathcal{O}(\mu^2)$ through the *parabolic recurrence method*.

2. Similarly, the periodic switching function-based approach leads also to a global convergence, provable by Lyapunov stability analysis, with residual oscillations around the extremum of order $\mathcal{O}(\varepsilon)$. Moreover, less restrictive assumptions, than in [2] are considered.

3. A generalization for dynamic maps with arbitrary relative degree is introduced in chapter 4, through a combination of time-scale and singular perturbation methods. The oscillations around the desired output are of order $\mathcal{O}(\sqrt{\eta}+\mu^2)$.

A limitation of using time-scaling method for compensation of relative degree, in addition to time dilation, is the fact that this method works for $\eta \to 0$, i.e, for fast unmodeled dynamics. Thus, strategies for nonlinear systems under the addition of slow unmodeled dynamics in view for relative degree compensation without compromising response time delay is the application of differentiators based on higher order sliding modes (HOSM).

5.1 Future Works

Every technique developed in this thesis lacks experimental validation to corroborate the theoretical results, although the presented simulations indicate their functionalities.

In [46], a detailed comparative experimental setup between multivariable gradient-based and Newton-based approaches (see section 1.2.2) is presented, applied to a photovoltaic (PV) Maximum Power Point Tracker (MPPT) problem, in which it is demonstrated that the Newton algorithm has better performance in terms of uniform and fast transients with low steady-state errors. Thus, we are encouraged to provide a similar experiment to validate our approach and compare to the aforementioned study.

In chapter 4, we solved the problem of arbitrary relative degree mitigation using the time-scaling and singular perturbation methods, which are valid for fast plant dynamics. However, we are limited to linear dynamic systems. Therefore, in the case of more general systems that include nonlinear and slow dynamics, one can introduce higher-order sliding modes (HOSM) differentiators [75] for the relative degree compensation.

Before the results presented here, we have proposed at CBA 2018 our first attempt to solve a problem of multivariable sliding mode based extremum seeking control via monitoring functions, where we defined a vector of reference trajectories that generate a vector of tracking errors and apply multiple monitoring functions to minimize independently each error, resulting in the optimization of all input variables of the objective function. However, this result and its demonstration (*proof*) have not yet been presented in the literature, and represent a possible research topic to be carried out, since the controller performance in terms of convergence rate of this scheme seems to be superior.

Similarly to the previous paragraph, and as mentioned in section 1.2.2, reference [52] presents an interesting approach to multivariable extremum seeking control via sliding modes and periodic switching function. However, the authors have presented a questionable demonstration and considered conservative assumptions, which makes it an open problem.

Finally, in the recent paper [76] was proposed a distributed extremum seeking control by using dynamic consensus algorithm via periodic switching function to optimize the total power produced in a wind farm. It is interesting to introduce an extremum seeking control via monitoring function and consensus algorithm in view to compare to such results and to our previous one (chapter 2).

Referências Bibliográficas

[1] GHAFFARI, A., KRSTIĆ, M., NESIĆ, D. "Multivariable Newton-based extremum seeking", *Automatica*, v. 48, n. 8, pp. 1759–1767, 2012.

[2] SALAMAH, Y. B., ÖZGUNER, U. "Sliding Mode Multivariable Extremum Seeking Control with Application to Wind Farm Power Optimization". In: *American Control Conference (ACC)*, pp. 5321 – 5326, Milwaukee, WI, USA, June 2018.

[3] BROWN, A., MÜLLER, S., DOBROTKOVA, Z. "Renewable energy: Markets and prospects by technology", *IEA Information Paper*, 2011.

[4] ATTA, K. T., JOHANSSON, A., GUSTAFSSON, T. "On-Line Optimization of Cone Crushers using Extremum-Seeking Control", *2013 IEEE Multi-conference on Systems and Control*, v. 42, n. 6, pp. 1054–1060, 2006.

[5] ARYIUR, K. B., , KRSTIĆ, M. *Real-Time Optimization by Extremum-Seeking Control*. Hoboken, New Jersey, John Wiley & Sons, 2003.

[6] UTKIN, V. I. *Sliding modes in control and optimization*. Communication and control engineering series. Berlin, New York, Springer-Verlag, 1992. ISBN: 3-540-53516-0.

[7] ZHANG, C., ARNOLD, D., GHODS, N., et al. "Source seeking with non-holonomic unicycle without position measurement and with tuning of forward velocity", *Systems & Control Letters*, v. 56, n. 3, pp. 245–252, 2007.

[8] OLIVEIRA, T. R., COSTA, L. R., CATUNDA, J. M. Y., et al. "Time-scaling based sliding mode control for Neuromuscular Electrical Stimulation under uncertain relative degrees", *Medical Engineering and Physics*, v. 44, pp. 53–62, 2017. doi: 10.1016/j.medengphy.2017.03.001.

[9] HARING, M., JOHANSEN, T. A. "Asymptotic Stability of Perturbation-Based Extremum-Seeking Control for Nonlinear Plants", *IEEE TRANSACTIONS ON AUTOMATIC CONTROL*, v. 62, n. 5, pp. 2302–2317, 2017.

[10] BAGHERI, M., KRSTI, M., NASERADINMOUSAVI, P. "Multivariable Extremum Seeking for Joint-Space Trajectory Optimization of a High-Degrees of Freedom Robot", *Journal of Dynamic Systems, Measurement, and Control*, v. 140, September 2018. doi: 10.1115/1.4040752].

[11] OLIVEIRA, T. R. *Rastreamento para Sistemas Incertos Fortemente Não-Lineares com Direção de Controle Desconhecida.* Tese de Doutorado, Programa de Eng. Elétrica, COPPE/UFRJ, Rio de Janeiro, 2010.

[12] KHALIL, H. K., ESFANDIARI, F. "Semi-global Stabilization of a Class of Nonlinear Systems Using Output Feedback", *IEEE TRANSACTIONS ON AUTOMATIC CONTROL*, v. 38, n. 9, pp. 1412–1415, 1993.

[13] AMINDE, N. O., OLIVEIRA, T. R., HSU, L. "Global output-feedback extremum seeking control via monitoring functions". In: *52nd IEEE Conference on Decision and Control*, pp. 1031–1036, Florence, Italy, December, 2013.

[14] OLIVEIRA, T. R., PEIXOTO, A. J., HSU, L. "Global real-time optimization by output-feedback extremum-seeking control with sliding modes", *Journal of Franklin Institute*, v. 349, n. 4, 2011.

[15] OLIVEIRA, T. R., AMINDE, N. O., HSU, L. "Monitoring Function based Extremum Seeking Control for Uncertain Relative Degrees with Light Source Seeking Experiments". In: *53rd IEEE Conference on Decision and Control*, pp. 3456–3462, Los Angels, California, December, 2014.

[16] HSU, L. "Private Correspondence", *France*, 1974.

[17] OLIVEIRA, T. R., PEIXOTO, A. J. "Extremum seeking control via sliding mode and periodic switching function applied to Raman optical amplifiers". In: *In Proc. american contr. conf.*, pp. 1397–1415, Montréal, Canada., 2012.

[18] ASELTINE, J. A., MANCINI, A., SARTURE, C. W. "A survey of adaptive control systems", *IRE Transactions on Automatic Control*, v. 6, n. 1, pp. 102–108, 1958.

[19] BENOSMAN, M. *Learning-Based Adaptive Control: An Extremum Seeking Approach - Theory and Applications.* 1 ed. Oxford, UK, Elsevier, 2016.

[20] IOANNOU, P., FIDAN, B. *Adaptive Control Tutorial.* 1 ed. Philadelphia, USA, The Society for Industrial and Applied Mathematics, 2006.

[21] ZHANG, C., ORDONEZ, R. *Extremum Seeking Control and Application: A Numerical Optimization-Based Approach*. London, UK, Springer-Verlag London Limited, 2012.

[22] CALLI, B., CAARLS, W., JONKER, P., et al. "Comparison of extremum seeking control algorithms for robotic applications". In: *Intelligent Robots and Systems (IROS), 2012 IEEE/RSJ International Conference on*, pp. 3195–3202, Vilamoura, Portugal, October, 2012.

[23] KRSTIĆ, M., WANG, H.-H. "Stability of extremum seeking feedback for general nonlinear dynamic systems", *Automatica*, v. 36, n. 4, pp. 595–601, 2000.

[24] ROTEA, M. M. "Analysis of multivariable extremum seeking algorithms", *American Contr. Conf.*, v. 1, n. 6, pp. 433–437, 2000.

[25] NESIC, D., TAN, Y., MAREELS, I. "On the Choice of Dither in Extremum Seeking Systems: a Case Study". In: *45TH IEEE Conference on Decision and Control*, pp. 2789–2794, 2006. doi: 10.1109/CDC.2006.377309.

[26] OLIVEIRA, T. R., KRSTIĆ, M., TSUBAKINO, D. "Multiparameter extremum seeking with output delays". In: *American Control Conference (ACC)*, pp. 152–158, July 2015. doi: 10.1109/ACC.2015.7170727.

[27] OLIVEIRA, T. R., KRSTIĆ, M., TSUBAKINO, D. "Extremum seeking subject to multiple and distinct input delays". In: *54th IEEE Conference on Decision and Control (CDC)*, pp. 5635–5641, Dec 2015.

[28] SCHEINKER, A., KRSTIĆ, M. *Model-Free Stabilization by Extremum Seeking*. Switzerland, Springer, 2017.

[29] Vaidyanathan, S., Lien, C.-H. (Eds.). *Applications of Sliding Mode Control in Science and Engineering*. Gewerbestrasse 11, 6330 Cham, Switzerland, Springer, 2017.

[30] UTKIN, V. I. "Variable structure systems with sliding modes", *In: IEEE Trans. Automat. Contr.*, v. 22, n. 7, pp. 212–222, 1977.

[31] SHTESSEL, Y., EDWARDS, C., FRIDMAN, L., et al. *Sliding Mode Control and Observation*. London, UK, Birkhäuser Basel, 2014.

[32] DA CUNHA, J., COSTA, R., HSU, L. "Design of a high performance variable structure position control of ROVs", *IEEE Journal of Oceanic Engineering*, v. 20, n. 1, pp. 42–55, 1995. doi: 10.1109/48.380247.

[33] SLOTINE, J.-J. E., LI, W. *Applied Nonlinear Control*. 1 ed. New Jersey, USA, Printice Hall, 1991.

[34] PERRUQUETTI, W., BARBOT, J. P. *Sliding Mode Control in Engineering*. New York, USA, Marcel Dekker, Inc, 2002.

[35] MUDGETT, D., MORSE, A. "Adaptive stabilization of linear systems with unknown high-frequency gains", *IEEE Transactions on Automatic Control*, v. 30, n. 6, pp. 549–554, 1985. doi: 10.1109/TAC.1985.1104006.

[36] YAN, L., HSU, L., COSTA, R. R., et al. "A variable structure model reference robust control without a prior knowledge of high frequency gain sign", *Automatica*, v. 44, n. 4, pp. 1036 – 1044, 2008. ISSN: 0005-1098. doi: 10.1016/j.automatica.2007.08.011.

[37] OLIVEIRA, T. R., PEIXOTO, A. J., NUNES, E. V. L., et al. "Control of uncertain nonlinear systems with arbitrary relative degree and unknown control direction using sliding modes", *Int. J. Adapt. Control Signal Process*, v. 21, pp. 692–707, 2007.

[38] HSU, L., COSTA, R. R. "Variable structure model reference adaptive control using only input and output measurement", *Int. J. Control*, v. 49, n. 2, pp. 399–416, 1989.

[39] HSU, L., DE ARAUJO, A., COSTA, R. "Analysis and design of I/O based variable structure adaptive control", *IEEE Transactions on Automatic Control*, v. 39, n. 1, pp. 4–21, 1994. doi: 10.1109/9.273335.

[40] HSU, L., LIZARRALDE, F., DE ARAUJO, A. "New results on output-feedback variable structure model-reference adaptive control: design and stability analysis", *IEEE Transactions on Automatic Control*, v. 42, n. 3, pp. 386–393, 1997. doi: 10.1109/9.557582.

[41] KOROVIN, S. K., UTKIN, V. I. "Using sliding modes in static optimization and nonlinear programming", *Automatica*, v. 10, n. 5, pp. 525–532, 1974.

[42] DRAKUNOV, S., ÖZGÜNER, U. "Optimization of Nonlinear System Output via Sliding Mode Approach", *Proceedings of the IEEE International Workshop on Variable Structure and Lyapunov Control of Uncertain Dynamical Systems*, pp. 61–62, 1992.

[43] OLIVEIRA, T. R., HSU, L., PEIXOTO, A. J. "Output-feedback global tracking for unknown control direction plants with application to extremum-

seeking control", *Automatica*, v. 47, n. 9, pp. 2029 – 2038, 2011. ISSN: 0005-1098.

[44] OLIVEIRA, T. R., COSTA, L. R., COSTA, A. V. "Extremum seeking applied to neuromuscular electrical stimulation", *IFAC-PapersOnLine*, v. 49, n. 32, pp. 188–193, 2016.

[45] TAN, Y., MOASE, W. H., MANZIE, C., et al. "Extremum seeking from 1922 to 2010". In: *29th Chinese Control Conference (CCC)*, pp. 14–26, Beijing, China, July, 2010.

[46] KRSTIĆ, M., GHAFFARI, A., SESHAGIRI, S. "Extremum Seeking for Wind and Solar Energy Applications", *Proceeding of the 11th World Congress on Intelligent Control and Automation*, pp. 6184–6193, 2014.

[47] XIAO, Y., LI, M. Y., SEEM, J. E. "Multi-variable Extremum Seeking Control for Mini-split Air-conditioning System", *International Refrigeration and Air Conditioning Conference*, pp. 1–13, 2014.

[48] WALSH, G. C. "On the application of multi-parameter extremum seeking control". In: *Proceedings of the American Control Conference*, pp. 411–415, Chicago, USA, June, 2000.

[49] ARYUR, K. B., KRSTIĆ, M. "Analysis and design of multivariable extremum seeking". In: *Proceedings of the American Control Conference*, pp. 2903–2908, Anchorage, USA, May, 2002.

[50] TAN, Y., NESIĆ, D., MAREELS, I. M. Y. "On non-local stability properties of extremum seeking control", *Automatica*, v. 42, n. 6, pp. 889–903, 2006.

[51] TAN, Y., MOASE, W., MANZIE, C., et al. "Extremum seeking from 1922 to 2010", *29th Chinese Control Conference*, pp. 14–26, 2010.

[52] TOLOUE, S. F., MOALLEM, M. "Multivariable Sliding-mode Extremum Seeking Control with Application to Alternator Maximum Power Point Tracking", *Transations on Industrial Electronics*, v. 64, n. 8, 2017.

[53] TEIXEIRA, M. C. M., ZAK, S. "Analog neural nonderivative optimizers", *Neural Networks, IEEE Transactions on*, v. 9, n. 4, pp. 629–638, 1998. ISSN: 1045-9227. doi: 10.1109/72.701176.

[54] PEIXOTO, A. J., OLIVEIRA, T. R., DIAS, D. P., et al. "Multivariable extremum-seeking by periodic switching functions with application to Raman optical amplifiers", *Control Engeneering Practice*, v. 96, 2020.

[55] CREABY, J., LI, Y., SEEM, J. E. "Maximizing Wind Turbine Energy Capture using Multivariable Extremum Seeking Control", *Wind Engineering*, 2009.

[56] FRIHAUF, P., KRSTIC, M., BASAR, T. "Nash Equilibrium Seeking in Noncooperative Games", *IEEE Transactions on Automatic Control*, v. 57, n. 5, pp. 1192–1207, May 2012. doi: 10.1109/TAC.2011.2173412.

[57] OLIVEIRA, T. R., KRSTIĆ, M., TSUBAKINO, D. "Extremum Seeking for Static Maps with Delays", *IEEE Transactions on Automatic Control*, v. 62, n. 4, pp. 1911–1926, 2017.

[58] LIU, W., HUO, X., LIU, J., et al. "Parameter Identification for a Quadrotor Helicopter Using Multivariable Extremum Seeking Algorithm", *International Journal of Control, Automation and Systems*, v. 16, n. 4, August 2018.

[59] OLIVEIRA, T. R., FEILING, J., KOGA, S., et al. "Multivariable e Extremum Seeking for PDE Dynamic Systems". In: *IEEE Transactions on Automatic Control*, pp. 1–8, 2020. doi: DOI:10.1109/TAC.2020.3005177.

[60] GHAFFARI, A., KRSTI, M., SESHAGIRI, S. "Power Optimization for Photovoltaic Microconverters Using Multivariable Newton-Based Extremum Seeking", *IEEE Transactions on Control Systems Technology*, v. 22, n. 6, pp. 2141–2149, Nov 2014. doi: 10.1109/TCST.2014.2301172.

[61] AMINDE, N. O., OLIVEIRA, T. R., HSU, L. "Multivariable extremum seeking control via cyclic search and monitoring function", *Int J Adapt Control Signal Process*, pp. 1–17, 2020. doi: 10.1002/acs.3151.

[62] TAN, Y., NESIĆ, D., I. M. Y. MAREELS, A. A. "On global extremum seeking in the presence of local extrema", *Automatica*, v. 45, n. 1, pp. 245–251, 2009.

[63] FILIPPOV, A. L. "Differential equations with discontinuous right-hand side", *Amer. Soc. Translations*, v. 42, pp. 199–231, 1964.

[64] KOKOTOVIC, P., KHALIL, H. K., OŔEILLY, J. *Singular Perturbation Methods in Control Analysis and Design*. Philadelphia, SIAM, 1999.

[65] UTKIN, V. I. *Sliding Modes and Their Application in Variable Structure Systems*. U.S.A., Moskow, 1978.

[66] YAN, L., HSU, L., COSTA, R. R., et al. "Variable Structure Model Reference Adaptive Control for Systems with Unknown High Frequency Gain". In: *Conference on Decision and Control*, Maui, Hawaii, USA, Dec 2003.

[67] OLIVEIRA, T. R., PEIXOTO, A. J., HSU, L. "Sliding mode control of uncertain multivariable nonlinear systems with unknown control direction via switching and monitoring function", *IEEE Trans. Automat. Contr.*, v. 55, n. 4, pp. 1028–1034, 2010.

[68] KASZKUREWICZ, E., BHAYA, A. *Matrix Diagonal Stability in Systems and Computation*. Boston, USA, Birkhauser, 2000 .

[69] ROSENBROCK, H. H. "An automatic method for finding the greatest or least value of a function", *The Computer Journal*, v. 3, pp. 175–184, 1960.

[70] YOUNG, K. D., UTKIN, V. I., ÖZGUNER, U. "A control engineer's guide to sliding mode control", *IEEE Transactions on Control Systems Technology*, v. 7, n. 3, pp. 328–342, 1999.

[71] HSU, L., OLIVEIRA, T. R., CUNHA, J. P. V. S. "Extremum Seeking Control via Monitoring Function and Time-Scaling for Plants of Arbitrary Relative Degree". In: *13th IEEE Workshop on Variable Structure Systems*, pp. 1–6, Nantes, France, 29 June-2 July 2014.

[72] KOKOTOVIĆ, P., KHALIL, H. K., O'REILLY, J. *Singular perturbation methods in control: analysis and design*. 2 ed. New York, SIAM, 1999.

[73] COSTA, R. R., HSU, L. "Unmodeled dynamics in adaptive control systems revisited", *Systems & Control Letters*, v. 16, n. 5, pp. 341–348, 1991.

[74] OLIVEIRA, T. R., RODRIGUES, V. H. P., FRIDMAN, L. "Generalized Model Reference Adaptive Control by Means of Global HOSM Differentiators", *IEEE Transactions on Automatic Control*, v. 64, n. 5, pp. 2053–2060, 2019. doi: 10.1109/TAC.2018.2862466.

[75] OLIVEIRA, T. R., ESTRADA, A., FRIDMAN, L. M. "Global and exact HOSM differentiator with dynamic gains for output-feedback sliding mode control", *Automatica*, v. 81, pp. 156–163, 2017.

[76] SALAMAH, Y. B., ÖZGUNER, U. "Distributed Extremum-Seeking for Wind Farm Power Maximization Using Sliding Mode Control", *Energies*, v. 14, n. 828, 2021. doi: https://doi.org/10.3390/en14040828.